

Supporting Information for

Calcium Ion Gradients Modulate the Zinc Affinity and Antibacterial Activity of Human Calprotectin

Megan Brunjes Brophy, Joshua A. Hayden, and Elizabeth M. Nolan*

Department of Chemistry, Massachusetts Institute of Technology, Cambridge MA 02139

*Corresponding author: lnolan@mit.edu

Phone: 617-452-2495

Fax: 617-324-0505

This Supporting Information section includes:

Complete ref. 54.....	S4
-----------------------	----

Supporting Experimental Methods

Cloning, Overexpression and Purification of CP and Mutants.....	S4
Site-Directed Mutagenesis.....	S7
Protein Mass Spectrometry.....	S8
Analytical Size Exclusion Chromatography.....	S8
Circular Dichroism Spectroscopy.....	S9
References.....	S9

Supporting Materials, Tables, and Figures

Design of the Synthetic Genes for Human S100A8 and Human S100A9.....	S10
Example ZP4 Two-Site Binding Model DYNAFIT Script.....	S11
Table S1. Primers Employed for S100A8.....	S12
Table S2. Primers Employed for S100A9.....	S13
Table S3. Templates and Primer Pairings Employed in Site-Directed Mutagenesis.....	S14
Table S4. Protein Nomenclature.....	S15
Table S5. Molecular Weights and Extinction Coefficients for CP.....	S16
Table S6. Molecular Weights and Extinction Coefficients for Subunits.....	S17
Table S7. Mass Spectrometry of CP and Mutants.....	S18
Table S8. Analytical SEC Retention Volumes.....	S19
Table S9. Metal-Ion Affinities for Bacterial Metal-Ion Transporters.....	S20
Figure S1. X-ray Crystal Structure of Human CP.....	S21
Figure S2. SDS-PAGE of CP-Ser Preparation.....	S22
Figure S3. SDS-PAGE of Purified Proteins.....	S23
Figures S4-S11. CD Spectra of CP-Ser and Mutants.....	S24

Figures S12-S26. Analytical Size Exclusion Chromatography (SEC) of CP and Mutants.....	S32
Figure S27. Ca(II)-Binding Titrations of CP and CP-Ser Monitored by SEC.....	S47
Figure S28. Thermal Denaturation of CP-Ser Monitored by CD.....	S48
Figure S29. Titration of CP-Ser Δ His ₃ Asp with Co(II) Monitored by Optical Absorption Spectroscopy.....	S49
Figure S30. Titration of CP-Ser with Co(II) in the Presence of Ca(II) Monitored by Optical Absorption Spectroscopy.....	S49
Figure S31. Co(II) EPR Power Saturations of CP-Ser, Δ His ₃ Asp and Δ His ₄	S50
Figure S32. CD Spectra of CP-Ser with Co(II).....	S51
Figure S33. Titration of CP-Ser with Co(II) and Zn(II) Monitored by Optical Absorption Spectroscopy.....	S52
Figure S34. Colorimetric Response of Mag-Fura-2 to Zn(II) in the presence of CP-Ser and the Mutants to Determine Zn:CP Stoichiometries.....	S53
Figure S35. Fluorescence Response of ZP4 to Zn(II) in the Presence of CP-Ser, Δ His ₃ Asp and Δ His ₄ and the Effect of Calcium.....	S54
Figures S36. ZP4 Titrations of ZP4 and $\Delta\Delta$ with Zn(II) in the Presence of Ca(II).....	S55
Figure S37. Colorimetric Response of Zincon to Zn(II) in the Presence of CP-Ser and Mutants to Determine Zn:CP Stoichiometries in the Presence of Ca(II).....	S56
Figure S38. Fluorescence of ZP4 in the presence of 1:2 Zn(II):CP-Ser.....	S57
Figure S39. CD Spectra of CP-Ser with Zn(II).....	S58
Figure S40. Antimicrobial Activity of CP-Ser Against <i>S. aureus</i>	S59
Figure S41. Effect of BME on Growth Inhibition by CP.....	S60
Figure S42. Structures of Colorimetric and Fluorimetric Sensors.....	S61

Complete ref 54

Jaroszewski, L.; Schwarzenbacher, R.; von Delft, F.; McMullan, D.; Brinen, L. S.; Canaves, J. M.; Dai, X. P.; Deacon, A. M.; DiDonato, M.; Elsliger, M. A.; Eshagi, S.; Floyd, R.; Godzik, A.; Grittini, C.; Grzechnik, S. K.; Hampton, E.; Levin, I.; Karlak, C.; Klock, H. E.; Koesema, E.; Kovarik, J. S.; Kreusch, A.; Kuhn, P.; Lesley, S. A.; McPhillips, T. M.; Miller, M. D.; Morse, A.; Moy, K.; Jie, O. Y.; Page, R.; Quijano, K.; Reyes, R.; Rezezadeh, F.; Robb, A.; Sims, E.; Spraggon, G.; Stevens, R. C.; van den Bedem, H.; Velasquez, J.; Vincent, J.; Wang, X. H.; West, B.; Wolf, G.; Xu, Q. P.; Hodgson, K. O.; Wooley, J.; Wilson, I. A., *Proteins* **2004**, *56* (3), 611-614.

Supporting Experimental Section

Cloning, Overexpression and Purification of CP and Mutants. Synthetic genes containing the *E. coli* optimized nucleotide sequences for human S100A8 and S100A9 were obtained in the pJ201 vector from DNA 2.0. The corresponding nucleotide and amino acid sequences are provided as Supporting Materials. Each synthetic gene contained a nucleotide sequence corresponding to a TEV cleavage site (ENLYFQG) at the 5' end of the S100A8/S100A9 gene. Plasmids pJ201-TEV-S100A8 and pJ201-TEV-S100A9 were each dissolved in 20 μ L of Milli-Q water and transformed (2 μ L aliquots) into chemically-competent *E. coli* TOP10 cells. Single colonies were selected and grown in 5 mL of LB media at 37 °C for 16 h. The plasmids were isolated from the overnight cultures by using a miniprep kit (Qiagen) and verified by DNA sequencing. The S100A8 and S100A9 genes were subcloned into pET41a without the TEV cleavage sites to afford pET41a-S100A8 and pET41a-S100A9. The S100A8 gene was PCR-amplified from pJ201-TEV-S100A8 by using the forward primer 5'-ggaattccatatgctgaccgagctgg-3' (*Nde*I restriction site underlined) and the reverse primer 5'-gatcctcgagttactcttatggctctcttcg-3' (*Xho*I restriction site underlined, stop codon in bold). The S100A9 gene was PCR-amplified from pJ201-TEV-S100A9 by using the forward primer 5'-ggaattccatatgacctgcaagatga-3' (*Nde*I restriction site underlined) and reverse primer 5'-

gatcctcgag**tt**acggagtagccttcgcccaga-3' (*Xho*I restriction site underlined, stop codon in bold). Polymerase chain reactions were performed with PfuTurbo DNA polymerase (Stratagene) and the amplified gene sequences were purified using an illustra GFX kit, digested with *Nde*I and *Xho*I (New England Biolabs), ligated into *Nde*I/*Xho*I-digested pET41a by using T4 DNA ligase (New England Biolabs), and transformed into chemically-competent *E. coli* TOP10 cells. Several single colonies from each transformation were selected and used to inoculate 5 mL of LB media. The cultures were grown to saturation, and a miniprep kit was used to isolate the pET41a-S100A8 and pET41a-S100A9 plasmids, the identities of which were verified by DNA sequencing.

The pET41a-S100A8 and pET41a-S100A9 expression plasmids were transformed into chemically-competent *E. coli* BL21(DE3) cells. Cultures from single colonies were grown to saturation in LB media containing 50 µg/mL kanamycin (37 °C, 150 or 175 rpm, t ~ 16 h), and freezer stocks were prepared by diluting the overnight cultures with an equal volume of 1:1 water/glycerol (sterile) and stored at -80 °C. For protein overexpression, over-night cultures were grown to saturation in LB media containing 50 µg/mL kanamycin (37 °C, 150 or 175 rpm, t ~ 16 h) and diluted 1:100 into fresh LB media containing 50 µg/mL kanamycin, incubated at 37 °C with shaking at 150 rpm, and induced with 500 µM IPTG at OD₆₀₀ ~ 0.6. The cultures were incubated at 37 °C for an additional 3-4 h (OD₆₀₀ ~ 1.5), and pelleted by centrifugation (4 200 rpm x 30 min, 4 °C). The cell pellets were transferred to pre-weighed 50-mL polypropylene centrifuge tubes, flash frozen in liquid N₂, and stored at -80 °C. These cultures were routinely grown in multiple 1- or 2-L portions contained in 2- or 4-L baffled flasks and stored as 1- or 2-L pellets. Approximately 2-3 g / L of *E. coli* cells (wet weight) were obtained from each preparation, and the cell pellets may be stored at -80 °C for at least three months.

The reconstitution and purification of heterodimeric CP was performed making several modifications to literature procedures.¹⁻³ All buffers were stored and maintained at 4 °C, and all purification steps were conducted on ice or in the cold room. In a typical purification, a single 1-L cell pellet of S100A8 and S100A9 was resuspended in ca. 30 mL of lysis buffer A (50 mM Tris-

HCl, 100 mM NaCl, 10 mM BME, 1.0 mM EDTA, 0.5% Triton-X, pH 8.0) and a 300- μ L aliquot of 100 mM PMSF was added to each tube to a final concentration of 1 mM. Resuspended S100A8 and S100A9 were combined in an ice-cold stainless steel beaker and the mixture was sonicated on ice (30 sec on, 10 sec off for 2.5 min; 40% amplitude). The crude lysate was clarified by centrifugation (14 000 rpm x 20 min, 4 °C) and the supernatant was decanted. The resulting cell pellet was resuspended in ca. 60 mL of lysis buffer A and a 600- μ L aliquot of 100 mM PMSF was added. The sonication and centrifugation steps were repeated, which yielded an off-white pellet. This pellet was resuspended in ca. 60 mL lysis buffer A and sonicated a third time. After centrifugation (14 000 rpm x 20 min, 4 °C), the resulting cell pellet was resuspended in ca. 120 mL of lysis buffer B (50 mM Tris-HCl, 100 mM NaCl, 10 mM BME, 4 M Gdn-HCl, pH 8.0) by either gentle stirring at 4 °C or by using a tissue homogenizer (Kontes). Once the pellet was completely solubilized, the clear solution was sonicated (30 sec on, 10 sec off for 5 min; 40% amplitude) on ice and centrifuged (14 000 rpm x 20 min, 4 °C). The resulting supernatant was transferred to a Spectropor3 3500 MWCO dialysis bag and dialyzed against 20 mM HEPES pH 8.0 buffer (3 x 4 L, 12-24 h per dialysis, 4 °C). A white precipitate formed during this step, and SDS-PAGE indicated that it mostly contained *E. coli* proteins (Figure S2). This mixture was centrifuged (14 000 rpm x 20 min, 4 °C) and the resulting supernatant was passed through a 0.45 μ m syringe filter and loaded into a 150-mL Superloop (GE Lifesciences). Chromatographic purification of CP was conducted by using an ÄKTA Purifier FPLC system (GE Lifesciences) housed in a 4 °C room. Crude heterodimeric CP was first purified by anion exchange chromatography by using a MonoQ 10/100 GL column and a gradient of 0-30 % B over 15 column volumes (eluent A, 20 mM HEPES, 10 mM BME, pH 8.0; eluent B, 20 mM HEPES, 1 M NaCl, 10 mM BME, pH 8). This step allowed for separation of CP from the S100A9 homodimer. Fractions containing CP (as determined by SDS-PAGE, 15% Tris-HCl gel) were pooled, concentrated to ~10 mL, and purified by gel filtration chromatography (20 mM HEPES, 100 mM NaCl, 10 mM BME, pH 8.0) using a HiLoad 26/600 S75 pg column (GE Lifesciences). Fractions containing pure CP were pooled, transferred to a Spectropor3 3500 MWCO dialysis bag, and

dialyzed against one liter of 20 mM HEPES, 10 mM BME, 100 mM NaCl, pH 8.0 containing ~10 g Chelex resin (Biorad) at 4 °C for ~12 h. The dialyzed protein was concentrated in an Amicon 10-kDa cut-off spin filter (3 750 rpm, 4 °C), aliquoted into sterile microcentrifuge tubes, flash frozen in liquid N₂, and stored at -80 °C. The yield for wild-type CP was routinely ~80 mg/2L (2 L refers to a prep where a 1-L cell pellet for S100A8 and a 1-L cell pellet for S100A9 were employed).

The overexpression, reconstitution, and purification of all heterodimeric CP mutants were conducted as described above for wild-type CP except that BME was omitted from all of the buffers. The yields for the mutant proteins ranged from ~10 mg/2L for $\Delta\Delta$ to ~45 mg/2L for CP-Ser and the metal-binding site mutants. The CP, CP-Ser, $\Delta\text{His}_3\text{Asp}$, ΔHis_4 , and $\Delta\Delta$ proteins were all overexpressed and purified multiple times, and samples from multiple preps were used throughout this work with high reproducibility. Tables S4-S6 include nomenclature, molecular weight and extinction coefficient data for wild-type CP and the mutant family members. For mutants such as $\Delta\Delta$ that were routinely obtained in lower yields, the purification scale was periodically increased to an 8-L scale (two 4-L pellets) using the same buffer volumes described above except that one extra lysis and sonication step prior to resuspension in lysis buffer B may be included and is recommended.

The wild-type and mutant proteins were routinely concentrated to >500 μM for storage purposes, aliquoted in 10- to 50- μL portions, and freeze-thawed only once. Prior to an experiment, the protein was thawed on ice and, if necessary, buffer exchanged as described below.

Site-Directed Mutagenesis. A modified Quick-Change site-directed mutagenesis protocol (Stratagene) was employed to generate the CP mutants (Table S4). The templates, primers and primer pairings are listed in Tables S1 and S2, respectively. The PCR protocol used for all mutagenesis reactions was: 95 °C for 30 min (1x); 55 °C for 1 min; 68 °C for 17 min (25x); 4 °C hold (1x). Following PCR amplification using PfuTurbo DNA polymerase, the template plasmid was digested with *DpnI* (New England Biolabs; 2 μL added to a 50 μL PCR

reaction in two 1- μ L aliquots at t = 0 and 1.5 h) for 3 h at 37 °C. The *DpnI* digests were transformed into chemically-competent *E. coli* TOP10 cells. Overnight cultures (5 mL, 50 μ g/mL kanamycin) were grown from single colonies and the purified plasmids were obtained by using a miniprep kit. The DNA sequences and presence of the desired mutation(s) were verified by DNA sequencing.

Protein Mass Spectrometry. An Agilent LC-MS system housing an Agilent 1260 series LC system and an Agilent 6230 TOF system outfitted with an Agilent Jetstream ESI source was employed for high-resolution electrospray impact mass spectrometry (ESI-MS). An Agilent Poroshell 300SB-C18 column (5 μ m pore size) and a denaturing protocol were utilized for all LC-MS analyses. Solvent A was 0.1% formic acid / water. Solvent B was 0.1% formic acid / acetonitrile. Protein samples (50 μ M) were prepared in 20 mM HEPES, 100 mM NaCl, pH 8.0 and a 2-5 μ L aliquot was injected onto the Poroshell column for each analysis. The S100A8 and S100A9 subunits were eluted by using a gradient of 0 to 65% B over 30 min with a flow rate of 0.2 mL/min. The resulting mass spectra were deconvoluted using the maximum entropy algorithm in MassHunter BioConfirm (Agilent).

Analytical Size Exclusion Chromatography. An ÄKTA Purifier (GE Lifesciences) outfitted with a 500- μ L sample loop was used for all analytical size exclusion chromatography (SEC). A Superdex 75 10/300 GL column (GE Lifesciences) was calibrated with a 100- μ L mixture of aprotinin (6.5 kDa, 3 mg/mL), ribonuclease A (13.7 kDa, 3 mg/mL), carbonic anhydrase (29 kDa, 3 mg/mL), ovalbumin (44 kDa, 4 mg/mL) and conalbumin (75 kDa, 3 mg/mL) obtained from GE Lifesciences. The mixture was buffered at pH 8 (20 mM HEPES, 150 mM NaCl). The carbonic anhydrase standard partially precipitated when added to the calibration mixture. The precipitate was pelleted by brief centrifugation, and the supernatant utilized for the column calibration. The dead volume of the column was determined with Blue Dextran 2000 (1 mg/mL) (GE Lifesciences). The partition coefficient, K_{av} , for each species was determined by the relationship:

$$K_{av} = (V_e - V_o) / (V_t - V_o)$$

where V_0 is the dead volume, V_e is the elution volume of the analyte, and V_t is the bed volume. K_{av} was plotted against the log of the molecular mass of each standard to obtain a linear calibration curve.

In a typical SEC experiment, a 200- to 250- μ L sample of 100 or 200 μ M CP was loaded into the sample loop. The column was pre-equilibrated with at least one column volume of running buffer (varied composition), the sample loop was subsequently emptied with 0.5 mL of running buffer, and the sample was eluted over one column volume at a flow rate of 0.5 mL/min. Analytical SEC experiments were conducted at either 4 °C or at room temperature as specified. Theoretical molecular weights were determined from K_{av} using the linear relationship provided by the calibration curve.

Circular Dichroism Spectroscopy. An Aviv Model 202 circular dichroism (CD) spectrometer thermostated at 25 °C was utilized to collect CD spectra. A 1-mm path-length quartz CD cell (Hellma) was employed for all CD measurements. Protein solutions (10 μ M, 250 – 300 μ L) were prepared by diluting an aliquot of a concentrated stock solution into 1 mM Tris-HCl, 500 mM EDTA, pH 8.5.¹ To determine the effect of Ca(II) on the protein fold, an aliquot of 100 mM Ca(II) was added to each sample to provide a final Ca(II) concentration of 1.5 – 2.5 mM and each CD spectrum was recorded ca. 3 min after Ca(II) addition. The CD spectra were collected from 260 – 195 nm at 1 nm intervals (3 sec averaging time, three independent scans per wavelength), and the data obtained from the three scans were averaged and plotted.

References

1. Hunter, M. J.; Chazin, W.J. *J. Biol. Chem.* **1998**, *273*, 12427-12435.
2. Kehl-Fie, T. E.; Chitayat, S.; Hood, M. I.; Damo, S.; Restrepo, N.; Garcia, C.; Munro, K. A.; Chazin, W. J.; Skaar, E. P. *Cell Host Microbe* 2011, *10*, 158-164.
3. Korndörfer, I. P.; Brueckner, F.; Skerra, A. *J. Mol. Biol.* **2007**, *370*, 887-898.

Supporting Materials

Design of the Synthetic Genes for Human S100A8 and Human S100A9

Synthetic genes for human S100A8 and human S100A9 were ordered from DNA 2.0 and optimized for *E. coli* codon usage. Both synthetic genes were designed to include an N-terminal TEV protease cleavage site (ENLYFQG) immediately adjacent to the start codon to provide TEV-S100A8 and TEV-S100A9. The TEV cleavage sequence was not utilized in this work, and the S100A8 and S100A9 genes were PCR-amplified as described in the main text.

In the nucleotide and amino acid sequences below, the sequences corresponding to the TEV sites are highlighted by italics and the start codons and corresponding Met residues are in bold font.

***E. coli* optimized nucleotide sequence for TEV-S100A8:**

GAGAATCTGTATTTCCAGGGTATGCTGACCGAGCTGGAGAAAGCGCTGAACTCCATTATCG
ACGTTTACCACAAATACAGCCTGATCAAGGGTAACTTTCACGCGGTCTATCGTGATGATCT
GAAGAAATTGCTGGAAACCGAATGCCCGCAGTACATCCGCAAAAAGGGCGCAGACGTGTG
GTTTAAGGAGTTGGACATTAACACGGATGGCGCTGTGAATTTCCAAGAATTCCTGATTCTG
GTCATCAAATGGGTGTTGCGGCCATAAGAAGAGCCACGAAGAGAGCCATAAAGAG

Translated sequence for TEV-S100A8:

ENLYFQGM L T E L E K A L N S I I D V Y H K Y S L I K G N F H A V Y R D D L K K L L E
T E C P Q Y I R K K G A D V W F K E L D I N T D G A V N F Q E F L I L V I K M G V A A H K K
S H E E S H K E

***E. coli* optimized nucleotide sequence for TEV-S100A9:**

GAGAATTTGTACTTTCAAGGCATGACCTGCAAGATGAGCCAGCTGGAACGCAATATCGAAA
CCATTATCAATACCTTCCACCAATACTCCGTCAAATTGGGTTCATCCGGACACGCTGAACCA
GGGCGAGTTTAAGGAGCTGGTTCGTAAAGATCTGCAGAACTTCTGAAGAAGGAGAACAA
GAACGAGAAAGTGATTGAACACATTATGGAGGATCTGGACACCAATGCAGACAAACAACTG
AGCTTTGAAGAGTTCATCATGCTGATGGCCCGTCTGACGTGGGCGAGCCACGAGAAAATG
CATGAAGGTGATGAAGGTCCGGGCCACCATCACAAACCGGGTCTGGGCGAAGGTACTCG

Translated sequence for TEV-S100A9:

ENLYFQGM T C K M S Q L E R N I E T I I N T F H Q Y S V K L G H P D T L N Q G E F K
E L V R K D L Q N F L K K E N K N E K V I E H I M E D L D T N A D K Q L S F E E F I M L M A
R L T W A S H E K M H E G D E G P G H H H K P G L G E G T P

Example ZP4 Two-Site Binding Model DYNAFIT Script

[task]

data = equilibria

task = fit

[mechanism]

$E + M \rightleftharpoons E.M$: Ka dissociation

$E.M + M \rightleftharpoons E.M.M$: Kb dissociation

$L + M \rightleftharpoons LM$: Kc dissociation

[constants]

Ka = 0.00035?, Kb = 0.005?, Kc = 0.00065

[concentrations]

E = 9.38 ?

L = 1.91

[responses]

L = 143, LM= 1268

[data]

plot titration

[equilibria]

directory ./examples/Mn/data2

extension txt

variable M

file zp4cp320data | concentration E = 9.38

response L = 143, LM= 1268

[output]

directory ./examples/constants

[end]

Table S1. Primers Employed for Sub-Cloning and Site-Directed Mutagenesis of S100A8.^a

Primer	Sequence
A8-1	5'-GGAATTCCATATGCTGACCGAGCTGG-3'
A8-2	5'-GATCCTCGAGTTACTCTTTATGGCTCTCTTCG-3'
C42S-1	5'-CTGGAAACCGAAAGCCGCGCAGTACATCC-3'
C42S-2	5'-GACCTTTGGCTTTCGGGCGTCATGTAGG-3'
H17A-1	5'-CGACGTTTACGCGAAATACAGCCTG-3'
H17A-2	5'-GCTGCAAATGCGCTTTATGTCCGAC-3'
H27A-1	5'-CAAGGGTAACTTTGCGGCGGTCTATCGTG-3'
H27A-2	5'-GTTCCCATGAAAAGCGCCGAGATAGCAC-3'
H83A-1	5'-CAAAATGGGTGTTGCGGCCGCGAAGAAGAGCCACGAAG-3'
H83A-2	5'-GTTTTACCCACAACGCCGGGCGTTCTTCTCGGTGCTTC-3'
H87A-1	5'-GCCCATAAGAAGAGCGCGGAAGAGAGCCATAAAG-3'
H87A-2	5'-CGGGTATTCTTCTCGCGCTTCTCTCGGTATTTC-3'
(H83A)-H87A-1	5'-GCCCGCGAAGAAGAGCGCGGAAGAGAGCCATAAAG-3'
(H83A)-H87A-2	5'-CGGCGCTTCTTCTCGCGCTTCTCTCGGTATTTC-3'

^a Underlined black codons indicate restriction sites. Bold codons indicate stop codons. The H83A mutation in the (H83A)-H87A primers is italicized and highlighted in blue. The codons containing the mutations are underlined and highlighted in red.

Table S2. Primers Employed for Sub-Cloning and Site-Directed Mutagenesis of S100A9.^a

Primer	Sequence
A9-1	5'-GGAATTCCATATGACCTGCAAGATGA-3'
A9-2	5'-GATCCTCGAGTTACGGAGTACCTTCGCCCAGA-3'
C3S-1	5'-CAAGGCATGACCAGCAAGATGAGCCAGC-3'
C3S-2	5'-GTTCCGTA CTGGTCGTTCTACTCGGTCG-3'
H20A-1	5'-CATTATCAATACCTTCGCAATACTCCGTCAAATTG-3'
H20A-2	5'-GTAATAGTTATGGAAGCGCTTATGAGGCAGTTTAAC-3'
D30A-1	5'-CAAATTGGGTCATCCGCGACGCTGAACCAGGGCGAG-3'
D30A-2	5'-GTTTAACCCAGTAGGCCTGCGACTTGGTCCCGCTC-3'
H91A-1	5'-GTCTGACGTGGGCGAGCGGAGAAAATGCATGAAGG-3'
H91A-2	5'-CAGACTGCACCCGCTCGCGCTCTTTTACGTA CTTC-3'
H95A-1	5'-GAGCCACGAGAAAATGGGAAGGTGATGAAGGTCC-3'
H95A-2	5'-CTCGGTGCTCTTTTACCTTCCACTACTTCCAGG-3'
(H91A)-H95A-1	5'-GAGCGGAGAAAATGGGAAGGTGATGAAGGTCC-3'
(H91A)-H95A-2	5'-CTCGCTCTTTTACCTTCCACTACTTCCAGG-3'

^a Underlined black codons indicate restriction sites. Bold codons indicate stop codons. The H91A mutation in the (H91A)-H95A primer is italicized and highlighted in blue. The codons containing the mutations are underlined and highlighted in red.

Table S3. Templates and Primer Pairings Employed in Site-Directed Mutagenesis.

Template	Product	Primer Pairing
pET41a-S100A8	pET41a-S100A8(C42S)	C42S-1, C42S-2
pET41a-S100A8(C42S)	pET41a-S100A8(C42S)(H17A)	H17A-1, H17A-2
pET41a-S100A8(C42S)	pET41a-S100A8(C42S)(H27A)	H27A-1, H27A-2
pET41a-S100A8(C42S)	pET41a-S100A8(C42S)(H83A)	H83A-1, H83A-2
pET41a-S100A8(C42S)	pET41a-S100A8(C42S)(H87A)	H87A-1, H87A-2
pET41a-S100A8(C42S)(H17A)	pET41a-S100A8(C42S)(H17A)(H27A)	H27A-1, H27A-2
pET41a-S100A8(C42S)(H38A)	pET41a-S100A8(C42S)(H83A)(H87A)	(H83A)-H87A-1, (H83A)-H87A-2
pET41a- S100A8(C42S)(H17A)(H27A)	pET41a- S100A8(C42S)(C17A)(H27A)(H83A)	H83A-1, H83A-2
pET41a- S100A8(C42S)(C17A)(H27A)(H83A)	pET41a- S100A8(C42S)(C17A)(H27A)(H83A)(H87A)	(H83A)-H87A-1, (H83A)-H87A-2
pET41a-S100A9	pET41a-S100A9(C3S)	C3S-1, C3S-2
pET41a-S100A9(C3S)	pET41a-S100A9(C3S)(H20A)	H20A-1, H20A-2
pET41a-S100A9(C3S)	pET41a-S100A9(C3S)(D30A)	D30A-1, D30A-2
pET41a-S100A9(C3S)	pET41a-S100A9(C3S)(H91A)	H91A-1, H91A-2
pET41a-S100A9(C3S)	pET41a-S100A9(C3S)(H95A)	H95A-1, H95A-2
pET41a-S100A9(C3S)(H20A)	pET41a-S100A9(C3S)(H20A)(D30A)	D30A-1, D30A-2
pET41a-S100A9(C3S)(H91A)	pET41a-S100A9(C3S)(H91A)(H95A)	(H91A)-H95A-1, (H91A)-H95A-2
pET41a- S100A9(C3S)(H20A)(D30A)	pET41a- S100A9(C3S)(H20A)(D30A)(H91A)	H91A-1, H91A-2
pET41a- S100A9(C3S)(H20A)(D30A)(H91A)	pET41a- S100A9(C3S)(H20A)(D30A)(H91A)(H95A)	(H91A)-H95A-1, (H91A)-H95A-2

Table S4. Protein Nomenclature.

Protein	Mutations	
	A8	A9
CP	Wild-type	Wild-type
CP-Ser	(C42S)	(C3S)
CP-Ser(H20A)	(C42S)	(C3S)(H20A)
CP-Ser(D30A)	(C42S)	(C3S)(D30A)
CP-Ser(H83A)	(C42S)(H83A)	(C3S)
CP-Ser(H87A)	(C42S)(H87A)	(C3S)
CP-Ser (D30A)(H83A)	(C42S)(H83A)	(C3S)(D30A)
CP-Ser Δ His ₃ Asp	(C42S)(H83A)(H87A)	(C3S)(H20A)(D30A)
CP-Ser(H17A)	(C42S)(H17A)	(C3S)
CP-Ser(H27A)	(C42S)(H27A)	(C3S)
CP-Ser(H91A)	(C42S)	(C3S)(H91A)
CP-Ser(H95A)	(C42S)	(C3S)(H95A)
CP-Ser (H27A)(H91A)	(C42S)(H27A)	(C3S)(H91A)
CP-Ser Δ His ₄	(C42S)(H17A)(H27A)	(C3S)(H91A)(H95A)
CP-Ser $\Delta\Delta$	(C42S)(H17A)(H27A)(H83A)(H87A)	(C3S)(H20A)(D30A)(H91A)(H95A)

Because all of the metal-binding site mutants are based on CP-Ser and include S100A8(C42S) and S100A9(C3S), the “CP-Ser” is routinely dropped from the mutant protein names throughout the Main Text and in the Supporting Information sections. In some instances when multiple mutants are being described or when conclusions are generalized to the wild-type protein, “CP” is utilized.

Table S5. Molecular Weights and Extinction Coefficients for CP and Mutant Proteins.

Protein	Molecular Weight (kDa) ^a $\alpha\beta$	ϵ_{280} ($M^{-1}cm^{-1}$) ^b $\alpha\beta$	Molecular Weight (kDa) ^a $\alpha_2\beta_2$	ϵ_{280} ($M^{-1}cm^{-1}$) ^b $\alpha_2\beta_2$
CP	24 058.4	18 450	48 116.8	36 900
CP-Ser	24 026.3	18 450	48 052.6	36 900
CP-Ser(H20A)	23 960.3	18 450	47 920.6	36 900
CP-Ser(D30A)	23 982.3	18 450	47 964.6	36 900
CP-Ser(H83A)	23 960.3	18 450	47 920.6	36 900
CP-Ser(H87A)	23 960.3	18 450	47 920.6	36 900
CP-Ser(D30A)(H83A)	23 916.2	18 450	47 814.5	36 900
CP-Ser Δ His ₃ Asp	23 784.1	18 450	47 568.2	36 900
CP-Ser(H17A)	23 960.3	18 450	47 920.6	36 900
CP-Ser(H27A)	23 960.3	18 450	47 920.6	36 900
CP-Ser(H91A)	23 960.3	18 450	47 920.6	36 900
CP-Ser(H95A)	23 960.3	18 450	47 920.6	36 900
CP-Ser(H27A)(H91A)	23 894.2	18 450	47 788.4	36 900
CP-Ser Δ His ₄	23 762.1	18 450	47 524.2	36 900
CP-Ser $\Delta\Delta$	23 519.9	18 450	47 021.8	36 900

^a Molecular weights were calculated by using the ProtParam tool available on the ExPASy server (<http://web.expasy.org/protparam>). ^b Extinction coefficients (280 nm) were calculated by using the ProtParam tool available on the ExPASy server (<http://web.expasy.org/protparam>).

Table S6. Molecular Weights and Extinction Coefficients for CP Subunits.

Subunit	Molecular Weight (Da) ^a	ϵ_{280} (M ⁻¹ cm ⁻¹) ^b
S100A8	10 834.5	11 460
S100A8 (C42S)	10 818.4	11 460
S100A8(C42S)(H17A)	10 752.3	11 460
S100A8(C42S)(H27A)	10 752.3	11 460
S100A8(C42S)(H83A)	10 752.3	11 460
S100A8(C42S)(H87A)	10 752.3	11 460
S100A8(C42S)(H17A)(H27A)	10 686.3	11 460
S100A8(C42S)(H83A)(H87A)	10 686.3	11 460
S100A8(C42S)(H17A)(H27A)(H83A)(H87A)	10 554.2	11 460
S100A9	13 241.9	6 990
S100A9(C3S)	13 255.9	6 990
S100A9(C3S)(H20A)	13 159.8	6 990
S100A9(C3S)(D30A)	13 181.9	6 990
S100A9(C3S)(H91A)	13 159.8	6 990
S100A9(C3S)(H95A)	13 159.8	6 990
S100A9(C3S)(H20A)(D30A)	13 115.8	6 990
S100A9(C3S)(H91A)(H95A)	13 093.9	6 990
S100A9(C3S)(H20A)(D30A)(H91A)(H95A)	12 983.7	6 990

^a Molecular weights were calculated by using the ProtParam tool available on the ExPASy server (<http://web.expasy.org/protparam>). ^b Extinction coefficients (280 nm) were calculated by using the ProtParam tool.

Table S7. Summary of Results from Mass Spectrometry of CP and Mutants.^a

Protein	S100A8 Calculated Mass (g/mol) ^b	S100A8 Observed Mass (g/mol) ^c	S100A9 Calculated Mass ± ^N Met (g/mol) ^d	S100A9 Observed Mass (g/mol)
CP	10 834.5	10 834.8	13 241.9 13 110.8 (-Met1)	n.f. ^e 13 111.0
CP-Ser	10 818.4	10 818.8	13 225.9 13 094.8 (-Met1)	13 226.0 13 095.0
CP-Ser(H20A)	10 818.4	10 818.8	13 159.8 13 028.7 (-Met1)	13 160.1 13 029.0
CP-Ser(D30A)	10 818.4	10 818.4	13 181.9 13 050.8 (-Met1)	13 181.8 13 050.9
CP-Ser(H83A)	10 752.3	10 752.6	13 225.9 13 094.8 (-Met1)	13 225.8 13 095.0
CP-Ser(H87A)	10 752.3	10 752.6	13 225.9 13 094.8 (-Met1)	13 225.9 13 095.0
CP-Ser(D30A)(H83A)	10 752.3	10 752.8	13 181.9 13 050.8 (-Met1)	13 182.0 13 050.9
CP-Ser ΔHis ₃ Asp	10 686.3	10 686.5	13 225.8 12 984.7 (-Met1)	n.f. 12 985.0
CP-Ser(H17A)	10 752.3	10 752.6	13 225.9 13 094.8 (-Met1)	13 225.7 13 095.0
CP-Ser(H27A)	10 752.3	10 752.8	13 225.9 13 094.8 (-Met1)	13 226.0 13 095.0
CP-Ser(H91A)	10 818.4	10 818.8	13 159.8 13 028.7 (-Met1)	13 159.8 13 029.0
CP-Ser(H95A)	10 818.4	10 818.6	13 159.8 13 028.7 (-Met1)	13 159.8 13 028.8
CP-Ser(H27A)(H91A)	10 752.3	10 752.5	13 159.8 13 028.7 (-Met1)	13 160.0 13 028.9
CP-Ser ΔHis ₄	10 686.3	10 686.5	13 093.8 12 962.7 (-Met1)	13 093.9 12 962.9
CP-Ser ΔΔ	10 554.2	10 554.3	12 983.7 12 852.6 (-Met1)	12 983.7 12 852.5

^a A denaturing protocol on an Agilent Poroshell 300SB-C18 column over a 0 – 65 % gradient of acetonitrile in 0.1 % formic acid was employed for LC-MS. ^b Molecular weights were calculated by using the ProtParam tool available on the ExPASy server (<http://web.expasy.org/protparam>). ^c Masses were calculated with the Agilent MassHunter BioConfirm software package. ^d The N-terminal methionine of S100A9 is sometimes cleaved during overexpression in *E. coli*. Masses are shown for the full-length and shortened forms of S100A9. ^e Mass not found following deconvolution of the raw data.

Table S8. Analytical SEC Retention Volumes in the Absence and Presence of Ca(II).^a

Protein	Retention Volume -Ca(II) (mL)	Calculated Molecular Weight (kDa)^b	Retention Volume +Ca(II) (mL)	Calculated Molecular Weight (kDa)
CP	10.8	37.0	10.1	49.0
CP-Ser	10.9	35.5	10.2	47.1
CP-Ser(H20A)	10.9	35.5	10.1	49.0
CP-Ser(D30A)	10.9	35.5	10.2	47.1
CP-Ser(H83A)	10.9	35.5	10.2	47.1
CP-Ser(H87A)	10.9	35.5	10.1	49.0
CP-Ser(D30A)(H83A)	10.9	35.5	10.2	47.1
CP-Ser Δ His ₃ Asp	10.8	37.0	10.2	47.1
CP-Ser(H17A)	11.0	34.1	10.1	49.0
CP-Ser(H27A)	11.0	34.1	10.1	49.0
CP-Ser(H91A)	11.0	34.1	10.1	49.0
CP-Ser(H95A)	10.9	35.5	10.1	49.0
CP-Ser(H27A)(H91A)	11.0	34.1	10.1	49.0
CP-Ser Δ His ₄	10.8	37.0	10.0	51.1
CP-Ser $\Delta\Delta$	10.8	37.0	10.0	51.1

^a Protein (100 μ M) was eluted over a S75 10/300 GL SEC column (GE Healthsciences) with 75 mM HEPES, 100 mM NaCl, pH 7.5 and a 0.5 mL/min flow rate. ^b Molecular weights were calculated with a calibration curve spanning a range of 6.5 – 75 kDa.

Table S9. Metal-ion Affinities for Select Bacterial Metal-ion Transporters and Metalloregulatory Proteins.

Protein	Role	Metal	Dissociation Constant (K_d)	Method ^a	Reference
SmtB	Metalloregulatory protein; <i>Synechococcus</i> PCC 7942	Zn(II)	$< 10^{-11}$ M	MF2; PAR	1
ZnuA	Periplasmic Zn(II) transporter; <i>E. coli</i>	Co(II)	5.9×10^{-9} M	PAR	2
		Zn(II)	$< 20 \times 10^{-9}$ M		
PsaA	Metal transport; <i>Streptococcus pneumoniae</i>	Mn(II)	3.3×10^{-9} M	ITC	3
TroA	Metal transport; <i>Streptococcus suis</i>	Zn(II)	231×10^{-9} M	ITC	4
		Mn(II)	254×10^{-9} M		
TroA	Metal transport; <i>Treponema pallidum</i>	Zn(II)	434×10^{-9} M	ITC	5
		Zn(II)	22.5×10^{-9} M		
YfeA	Soluble metal transport protein; <i>Yersinia pestis</i>	Mn(II)	7.1×10^{-9} M	ITC	6
		Mn(II)	17.8×10^{-9} M		
		Zn(II)	6.6×10^{-9} M		

^a MF2 = metal-ion competition titration with Mag-Fura-2; PAR = metal-ion competition titration with 4-(2-pyridylazo)resorcinol; ITC = metal-ion binding titration by isothermal titration calorimetry.

References for Table 9

1. VanZile, M. L.; Cospers, N. J.; Scott, R. A.; Giedroc, D.P. *Biochemistry* **2000**, *39*, 11818-11829.
2. Yatsunyk, L.A.; Easton, J. A.; Kim, L. R.; Sugarbaker, S. A.; Bennett, B.; Breece, R. M.; Vorontsov, I. I.; Tierney, D. L.; Crowder, M. W.; Rosenzweig, A. C. *J. Biol. Inorg. Chem.* **2008**, *13*, 271-288.
3. McDevitt, C.A.; Ogunniyi, A. D.; Valkov, E.; Lawrence, M. C.; Kobe, B.; McEwan, A. G.; Paton, J. C. *PLoS Pathog.* **2011**, *7*, e1002357.
4. Zheng, B.; Zhang, Q. M.; Gao, J.; Han, H. M.; Li, M.; Zhang, J. R.; Qi, J. X.; Yan, J. H.; Gao, G. F. *PLoS One.* **2011**, *6*, e19510.
5. Desrosiers, D.C.; Sun, Y. C.; Zaidi, A. A.; Eggers, C. H.; Cox, D. L.; Radolf, J. D. *Mol. Microbiol.* **2007**, *65*, 137-152.
6. Desrosiers, D.C.; Bearden, S. W.; Mier, I.; Abney, J.; Paulley, J. T.; Fetherston, J. D.; Salazar, J. C.; Radolf, J. D.; Perry, R. D. *Infect. Immun.* **2010**, *78*, 5163-5177.

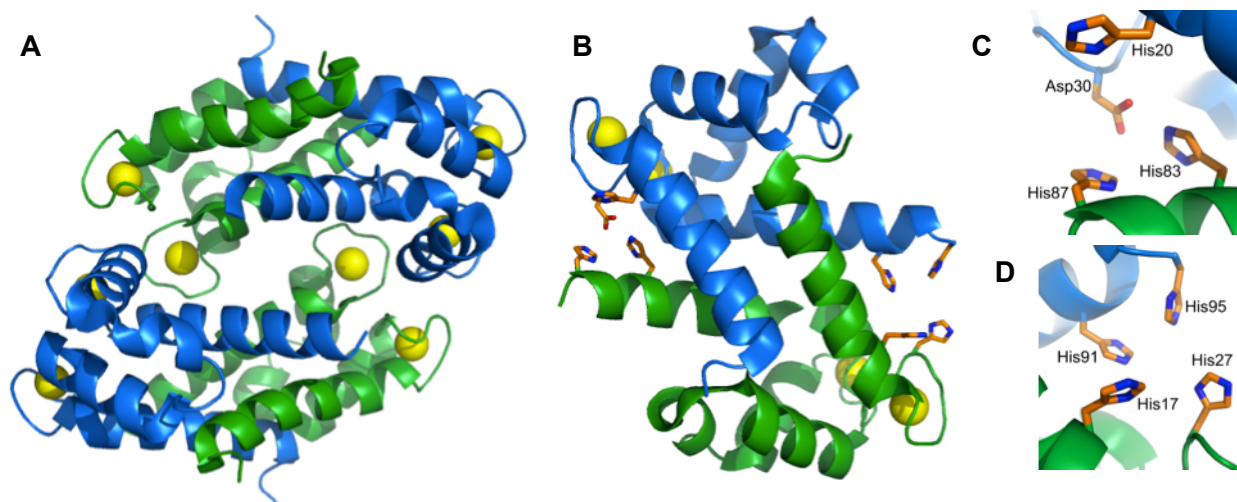


Figure S1. X-ray crystal structure of human CP ($\alpha_2\beta_2$) (PDB: 1XK4) reported by Skerra and co-workers (*J. Mol. Biol.* **2007**, *370*, 887-898). The recombinant protein employed in the crystallization was CP-Ser and it crystallized as the heterotetramer in the presence of Ca(II). S100A8 (α) is depicted in green and S100A9 (β) is shown in blue. The Ca(II) ions are represented as yellow spheres. The S100A9 C-terminal tail (residues 92-114 and 96-114 of each A9 subunit) was disordered and is not shown. (a) The $\alpha_2\beta_2$ heterotetramer. (b) One heterodimeric unit of the structure presented in a is shown in a different orientation to show the putative His₃Asp (site 1) and His₄ (site 2) metal-binding sites. This depiction includes the Ca(II) ions and is used as a model for the apo heterodimer in this work. S100A8 and S100A9 each contribute two residues to each metal-binding site. (c) Close-up view of the His₃Asp site. (d) Close-up view of the His₄ site.

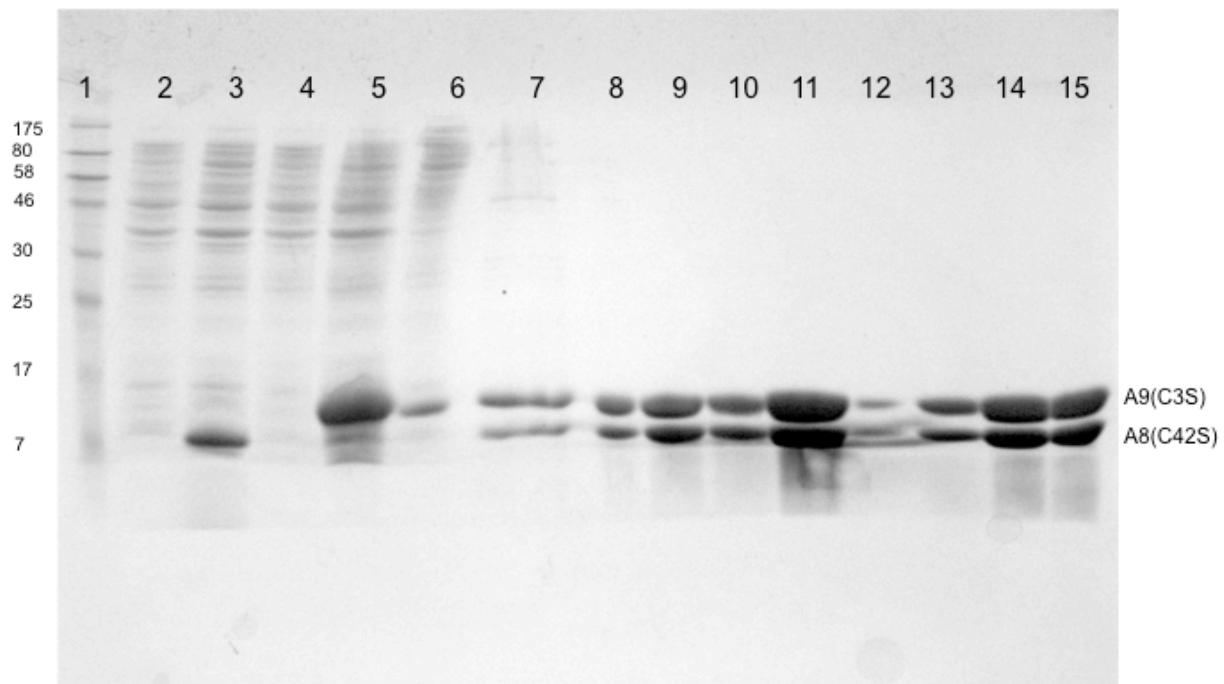


Figure S2. SDS-PAGE (15% Tris-HCl gel) of samples from a representative preparation of CP-Ser. S100A8 is 10.8 kDa and S100A9 is 13.2 kDa. Lane 1: P7708S pre-stained gel ladder (New England Biolabs). Lanes 2 and 3: overexpression of S100A8(C42S) showing pre- and post-induction samples. Lanes 4 and 5: overexpression of S100A9(C3S) showing pre- and post-induction samples. Lane 6: the soluble fraction after combining the A8 and A9 cell pellets and lysis. Lane 7: the insoluble fraction after cell lysis. Lane 8: Soluble CP-Ser after refolding. Lanes 9-11: Fractions containing CP-Ser obtained from anion-exchange chromatography. Lanes 12-15: fractions containing pure CP-Ser from gel-filtration chromatography.

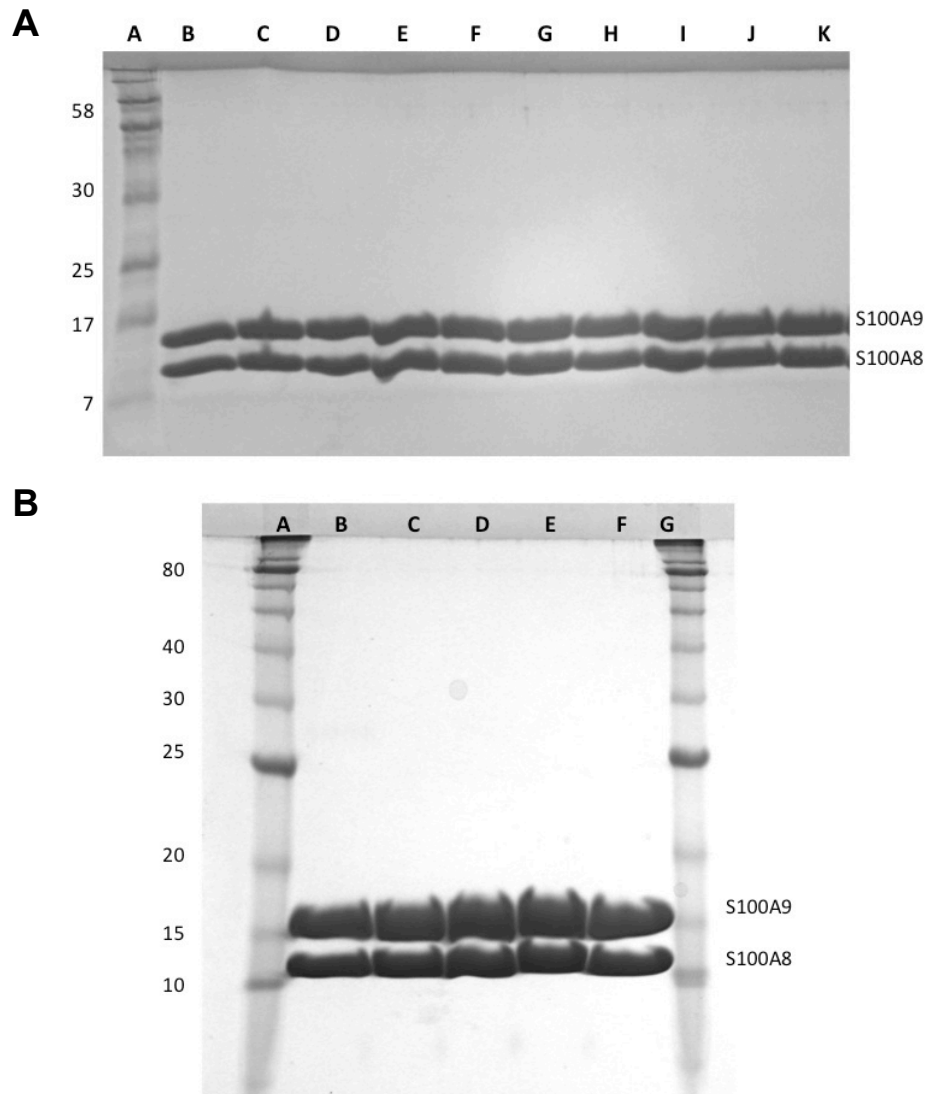


Figure S3. SDS-PAGE (15% Tris-HCl gel) of purified proteins employed in this study. S100A8 is 10.8 kDa and S100A9 is 13.2 kDa. Top panel A: Single and double mutants of the His₃Asp and His₄ sites. (A) P7708S pre-stained gel ladder; (B) CP-Ser(H20A); (C) CP-Ser(D30A); (D) CP-Ser(H83A); (E) CP-Ser(H87A); (F) CP-Ser(D30A)(H83A); (G) CP-Ser(H17A); (H) CP-Ser(H27A); (I) CP-Ser(H91A); (J) CP-Ser(H95A); (K) CP-Ser(H27A)(H91A). Bottom panel B: Wild-type CP and metal-binding site mutants. (A) P7710S pre-stained gel ladder; (B) CP; (C) CP-Ser; (D) CP-Ser Δ His₃Asp; (E) CP-Ser Δ His₄; (F) CP-Ser $\Delta\Delta$; (G) P7710S.

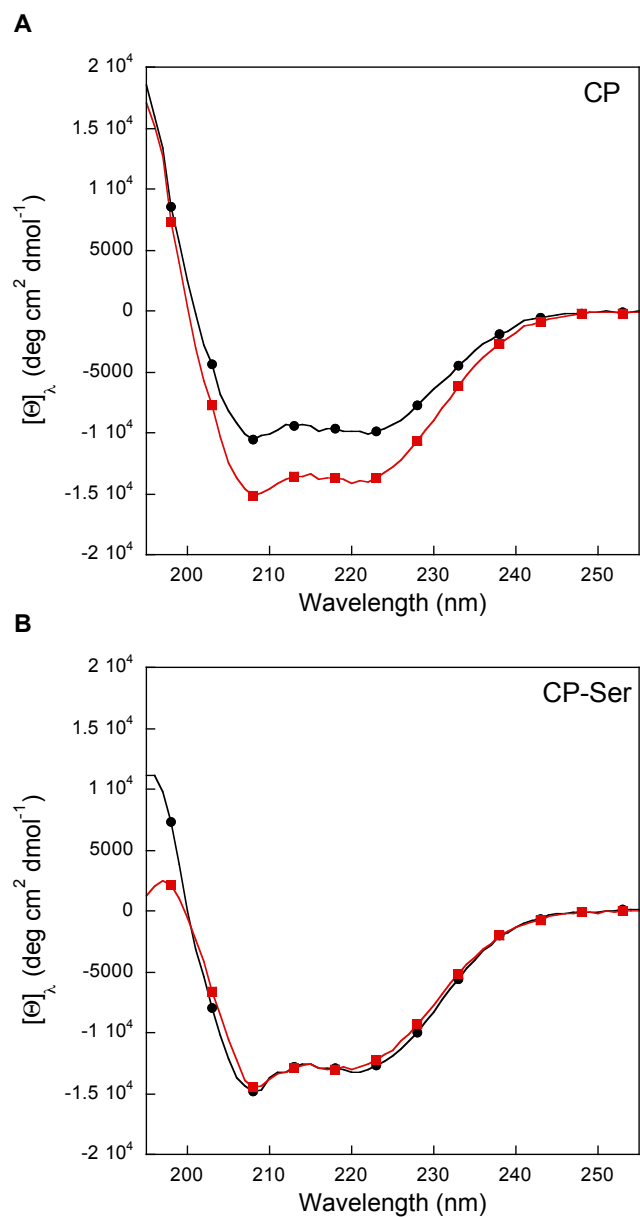


Figure S4. CD spectra of 10 μ M CP and CP-Ser in the absence (black circles) and presence (red squares) of 2 mM Ca(II) (1 mM Tris-HCl, 0.5 mM EDTA, pH 8.5, T = 25 $^{\circ}$ C).

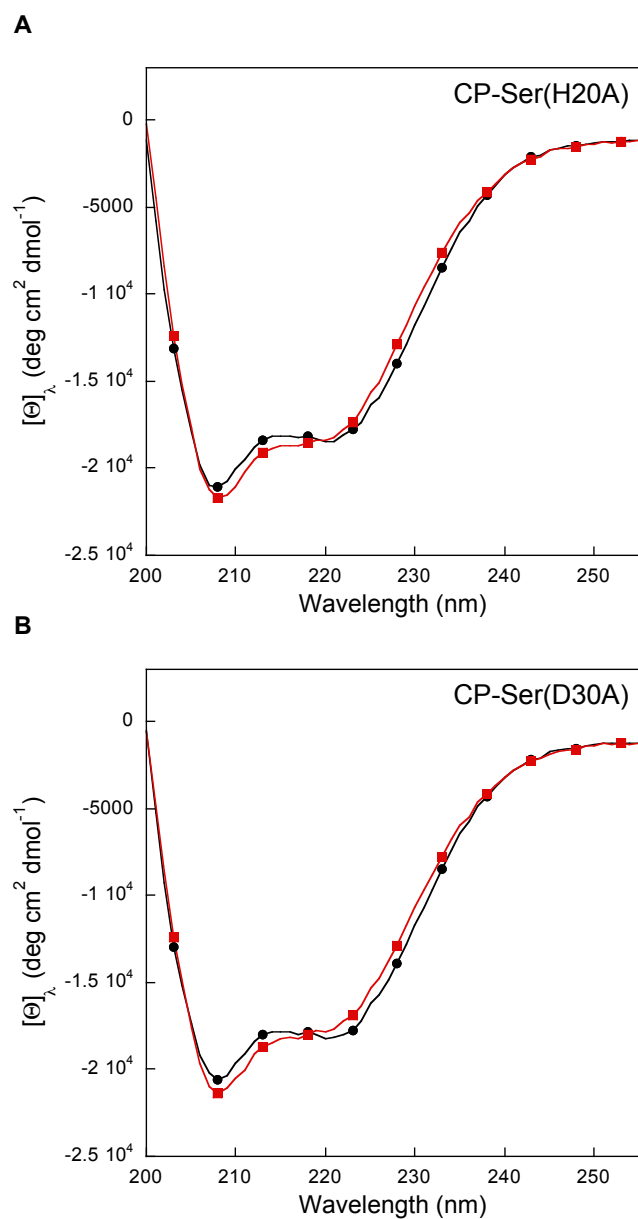


Figure S5. CD spectra of 10 μM CP-Ser(H20A) and CP-Ser(D30A) in the absence (black circles) and presence (red squares) of 2 mM Ca(II) (1 mM Tris-HCl, 0.5 mM EDTA, pH 8.5, T = 25 $^{\circ}\text{C}$). The data was collected only to 200 nm because of a high dynode at shorter wavelengths.

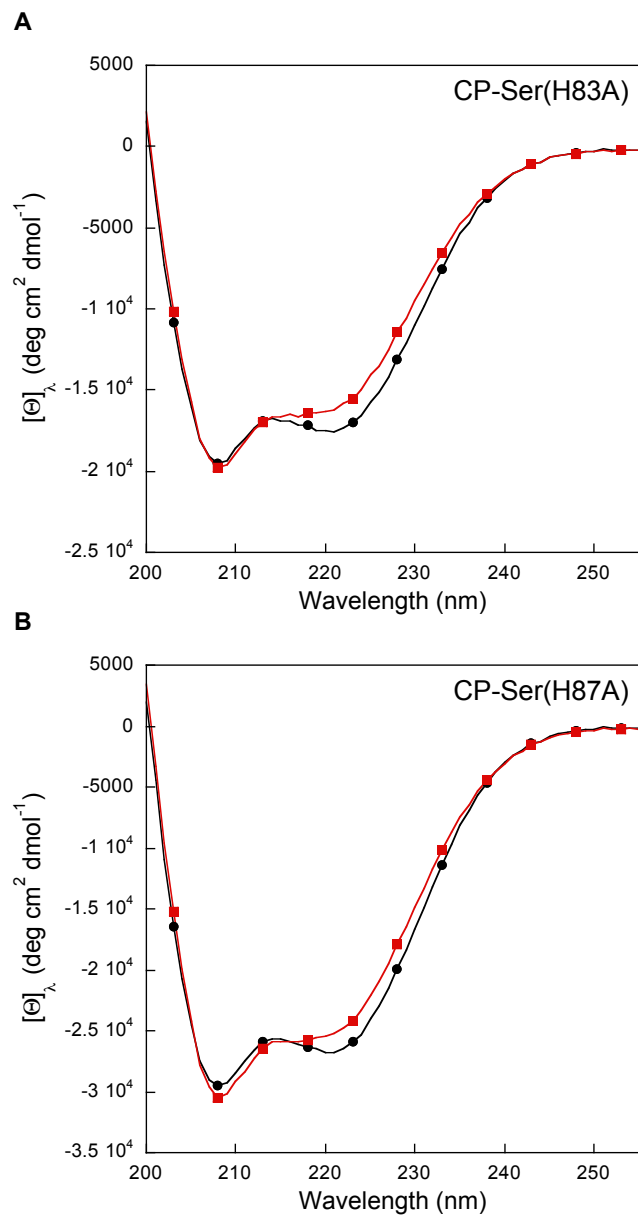


Figure S6. CD spectra of 10 μ M CP-Ser(H83A) and CP-Ser(H87A) in the absence (black circles) and presence (red squares) of 2 mM Ca(II) (1 mM Tris-HCl, 0.5 mM EDTA, pH 8.5, T = 25 °C). The data was collected only to 200 nm because of a high dynode at shorter wavelengths.

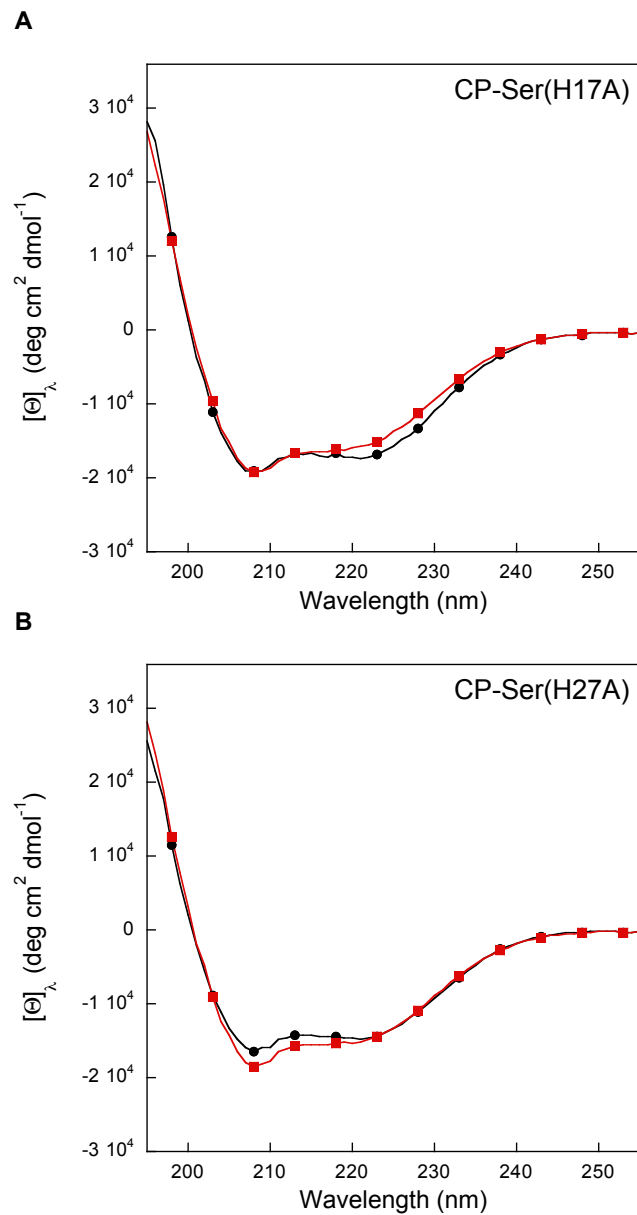


Figure S7. CD spectra of 10 μ M CP-Ser(H17A) and CP-Ser(H27A) in the absence (black circles) and presence (red squares) of 2 mM Ca(II) (1 mM Tris-HCl, 0.5 mM EDTA, pH 8.5, T = 25 °C).

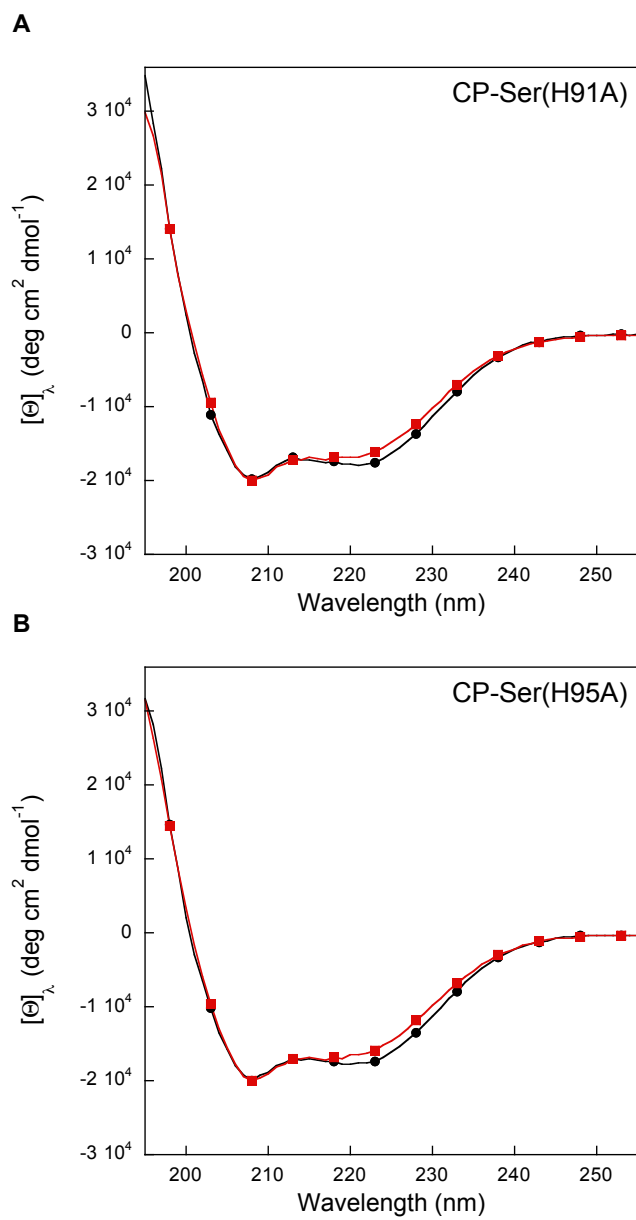


Figure S8. CD spectra of 10 μ M CP-Ser(H91A) and CP-Ser(H95A) in the absence (black circles) and presence (red squares) of 2 mM Ca(II) (1 mM Tris-HCl, 0.5 mM EDTA, pH 8.5, T = 25 °C).

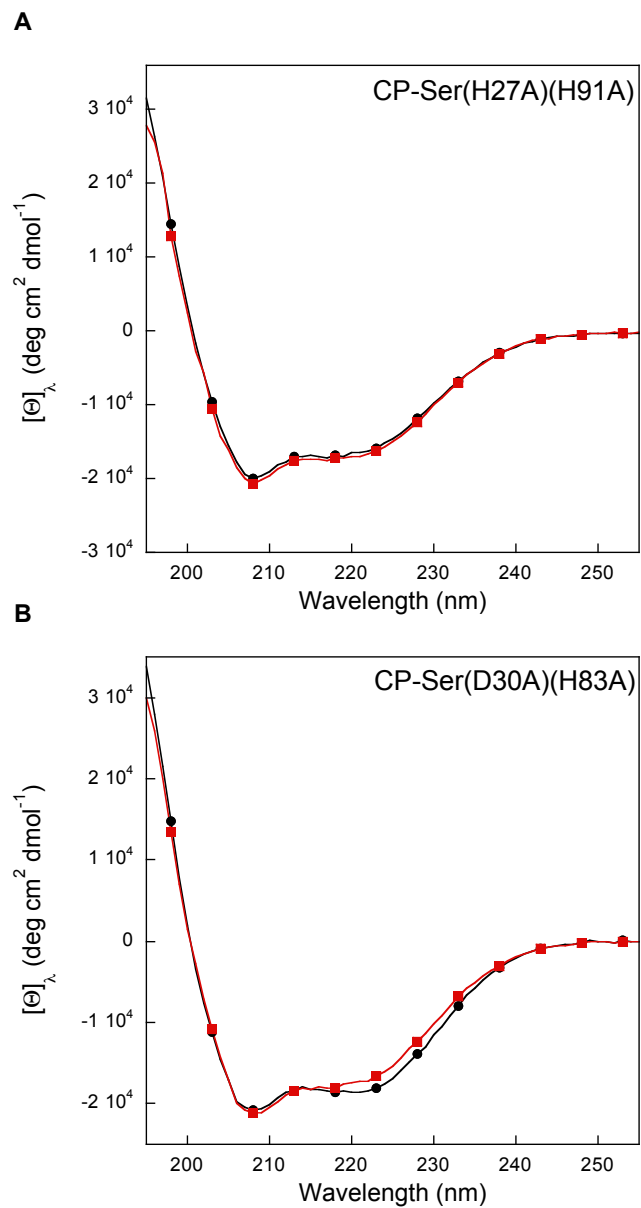


Figure S9. CD spectra of 10 μ M CP-Ser(H27A)(H91A) and CP-Ser(D30A)(H83A) in the absence (black circles) and presence (red squares) of 2 mM Ca(II) (1 mM Tris-HCl, 0.5 mM EDTA, pH 8.5, T = 25 °C).

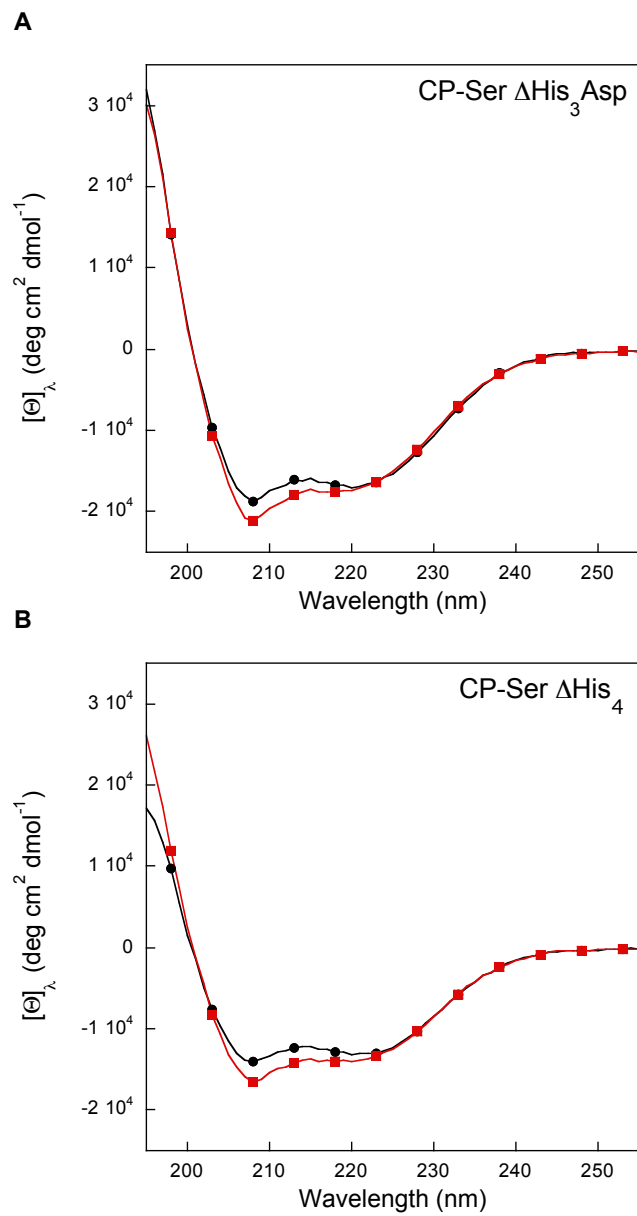


Figure S10. CD spectra of 10 μ M CP-Ser Δ His₃Asp and CP-Ser Δ His₄ in the absence (black circles) and presence (red squares) of 2 mM Ca(II) (1 mM Tris-HCl, 0.5 mM EDTA, pH 8.5, T = 25 °C).

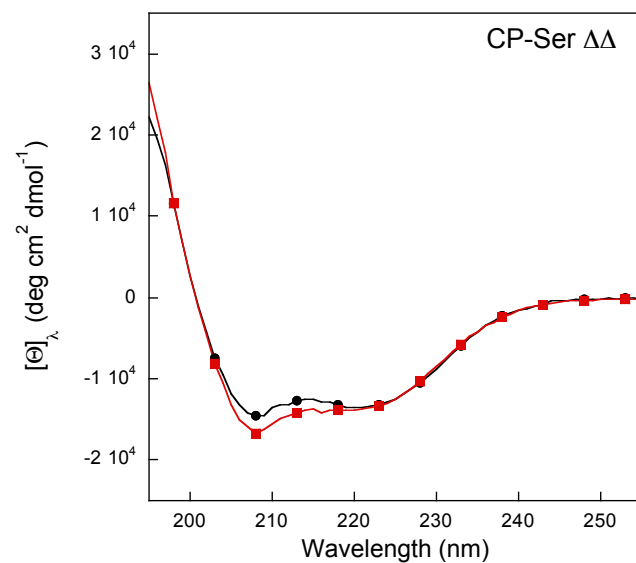


Figure S11. CD spectra of 10 μ M CP-Ser $\Delta\Delta$ in the absence (black circles) and presence (red squares) of 2 mM Ca(II) (1 mM Tris-HCl, 0.5 mM EDTA, pH 8.5, T = 25 °C).

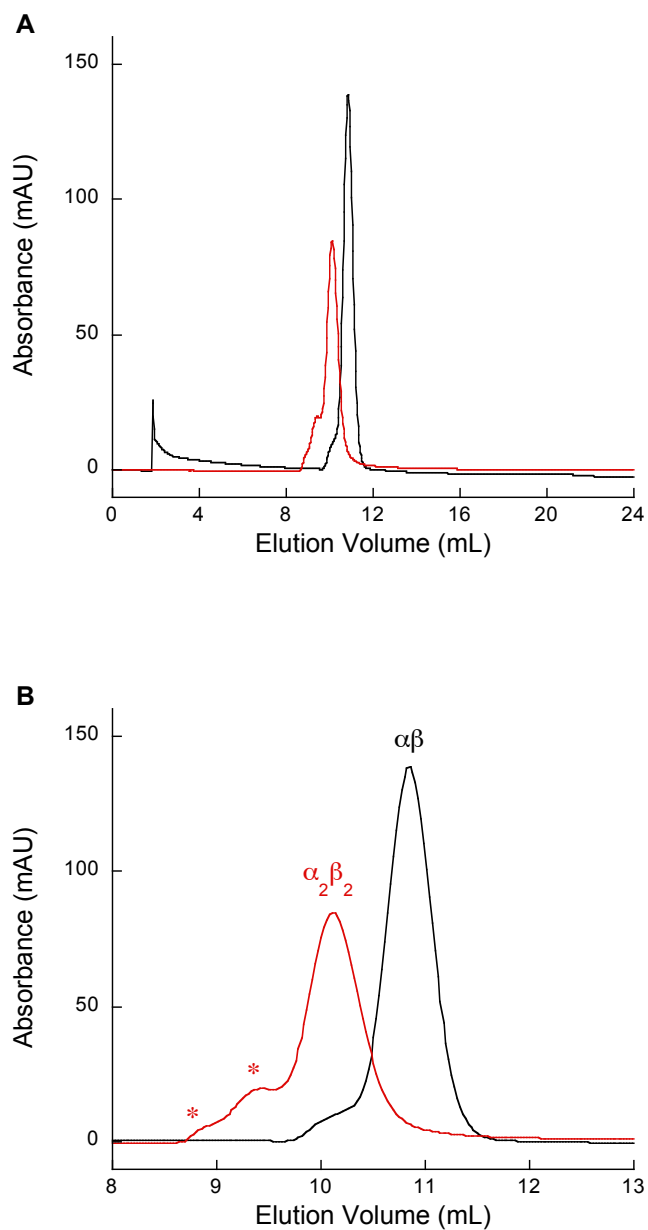


Figure S12. Analytical size exclusion chromatography of 100 μM CP in the absence (black) and presence (red) of 2 mM Ca(II) in the running buffer (75 mM HEPES, 100 mM NaCl, pH 7.5). **(A)** Full chromatograms. **(B)** Expansion. The red stars indicate Ca(II)-dependent peaks attributed to higher-order oligomers. Absorption was monitored at 280 nm at room temperature. Elution volumes are listed in Table S8.

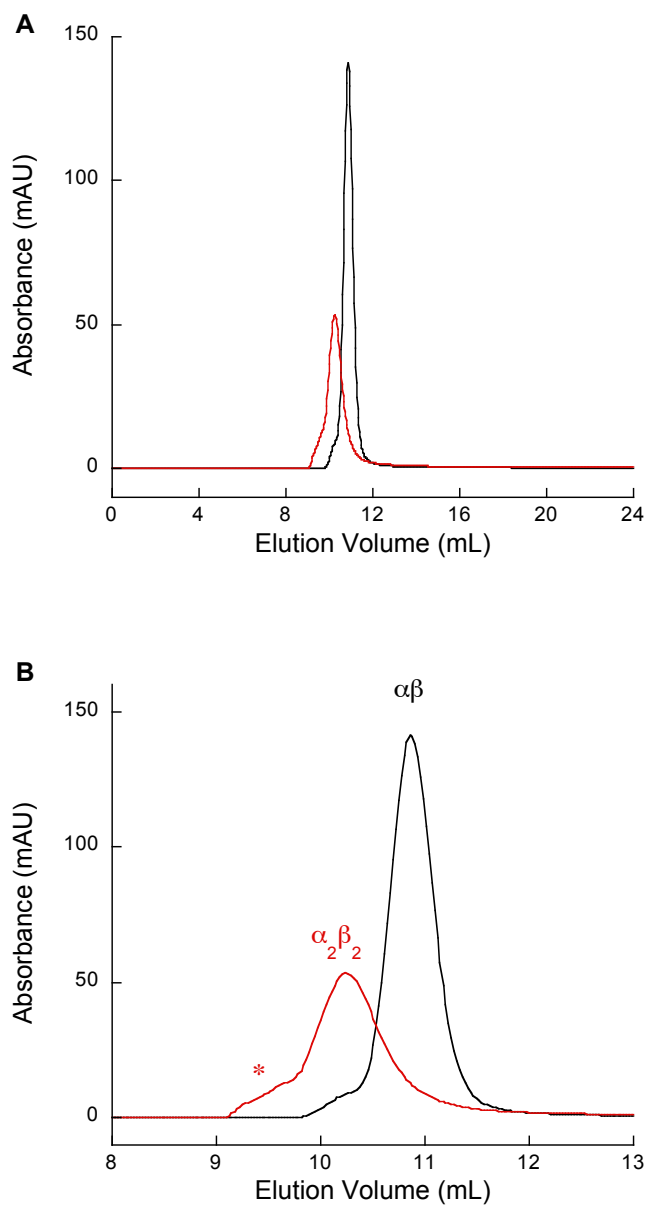


Figure S13. Analytical size exclusion chromatography of 100 μM CP-Ser in the absence (black) and presence (red) of 2 mM Ca(II) in the running buffer (75 mM HEPES, 100 mM NaCl, pH 7.5). **(A)** Full chromatograms. **(B)** Expansion. The red star indicates Ca(II)-dependent peaks attributed to higher-order oligomers. Absorption was monitored at 280 nm and room temperature. Elution volumes are listed in Table S8.

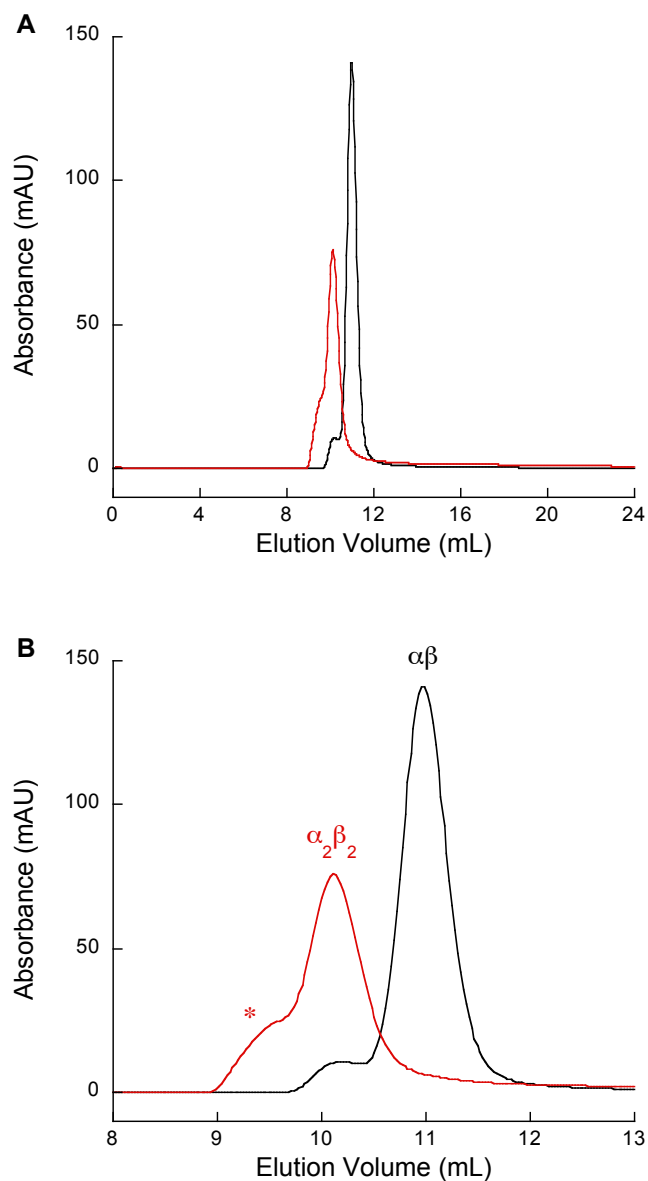


Figure S14. Analytical size exclusion chromatography of 100 μ M CP-Ser(H17A) in the absence (black) and presence (red) of 2 mM Ca(II) in the running buffer (75 mM HEPES, 100 mM NaCl, pH 7.5). **(A)** Full chromatograms. **(B)** Expansion. The red star indicates Ca(II)-dependent peaks attributed to higher-order oligomers. Absorption was monitored at 280 nm and room temperature. Elution volumes are listed in Table S8.

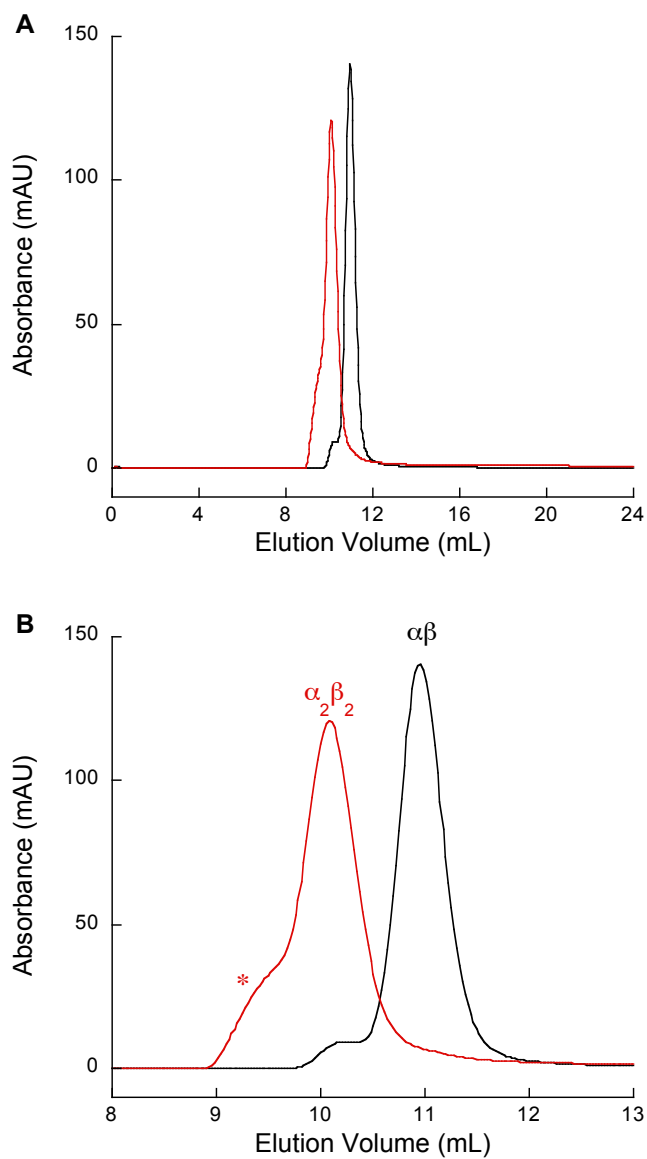


Figure S15. Analytical size exclusion chromatography of 100 μ M CP-Ser(H27A) in the absence (black) and presence (red) of 2 mM Ca(II) in the running buffer (75 mM HEPES, 100 mM NaCl, pH 7.5). **(A)** Full chromatograms. **(B)** Expansion. The red star indicates Ca(II)-dependent peaks attributed to higher order oligomers. Absorption was monitored at 280 nm and room temperature. Elution volumes are listed in Table S8.

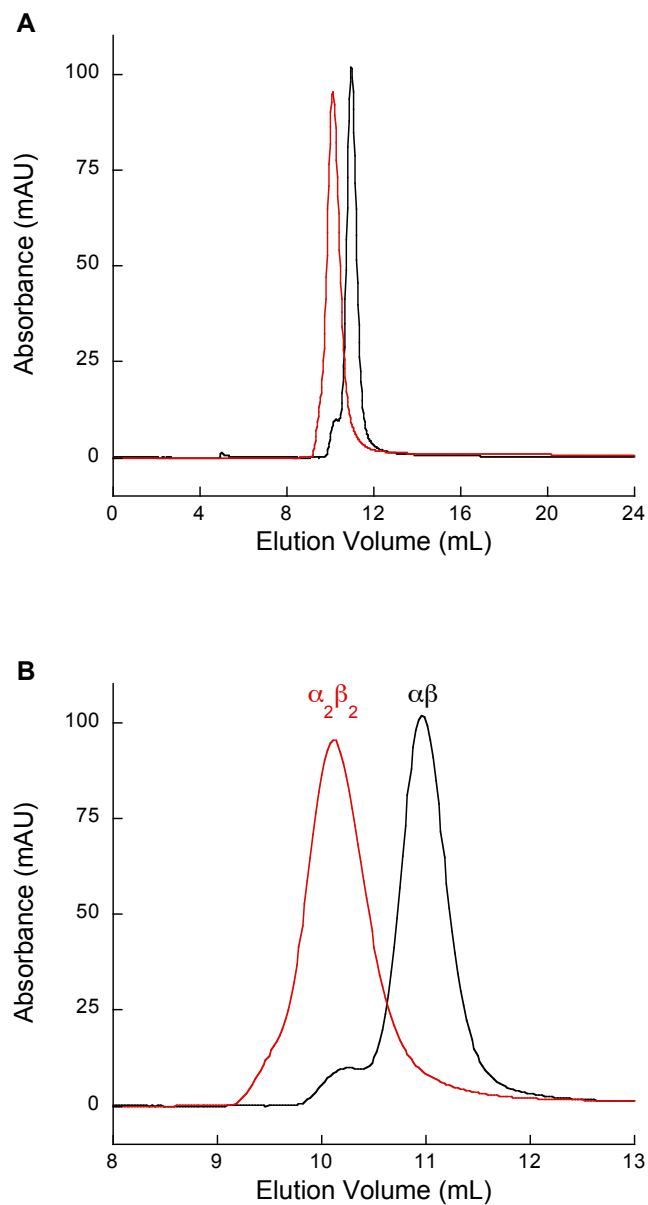


Figure S16. Analytical size exclusion chromatography of 100 μ M CP-Ser(H91A) in the absence (black) and presence (red) of 2 mM Ca(II) in the running buffer (75 mM HEPES, 100 mM NaCl, pH 7.5). **(A)** Full chromatograms. **(B)** Expansion. Absorption was monitored at 280 nm and room temperature. Elution volumes are listed in Table S8.

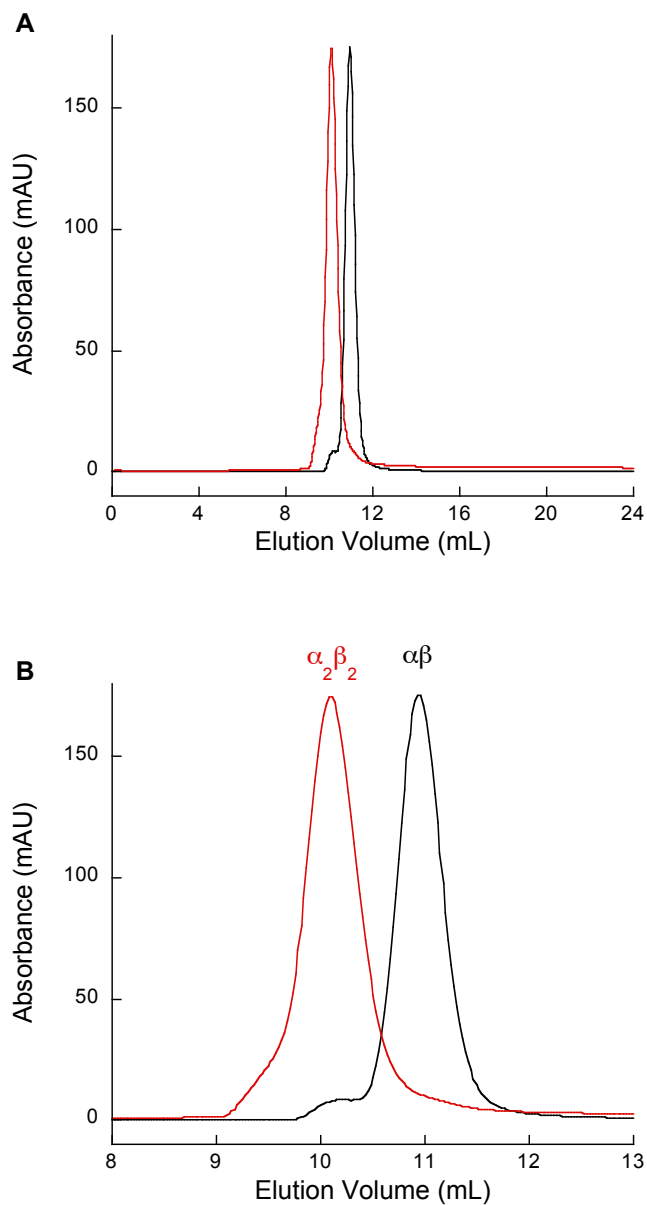


Figure S17. Analytical size exclusion chromatography of 100 μ M CP-Ser(H95A) in the absence (black) and presence (red) of 2 mM Ca(II) in the running buffer (75 mM HEPES, 100 mM NaCl, pH 7.5). **(A)** Full chromatograms. **(B)** Expansion. The red star indicates Ca(II)-dependent peaks attributed to higher-order oligomers. Absorption was monitored at 280 nm and room temperature. Elution volumes are listed in Table S8.

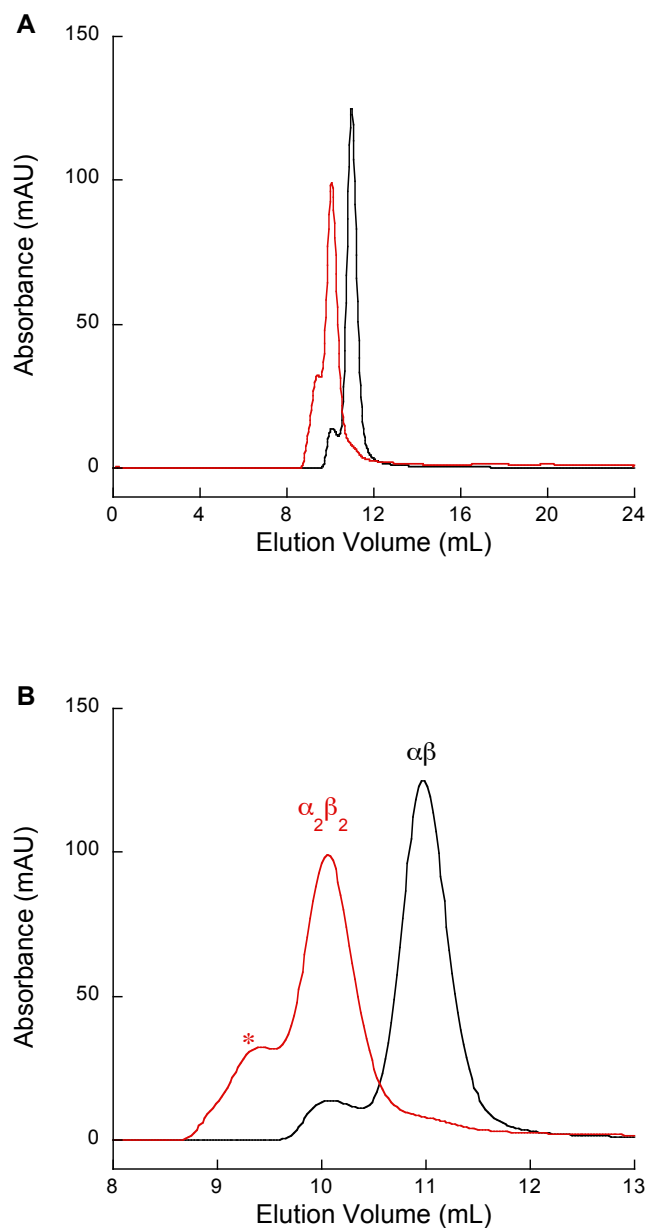


Figure S18. Analytical size exclusion chromatography of 100 μM CPSer(H27A)(H91A) in the absence (black) and presence (red) of 2 mM Ca(II) in the running buffer (75 mM HEPES, 100 mM NaCl, pH 7.5). **(A)** Full chromatograms. **(B)** Expansion. The red star indicates Ca(II)-dependent peaks attributed to higher-order oligomers. Absorption was monitored at 280 nm and room temperature. Elution volumes are listed in Table S8.

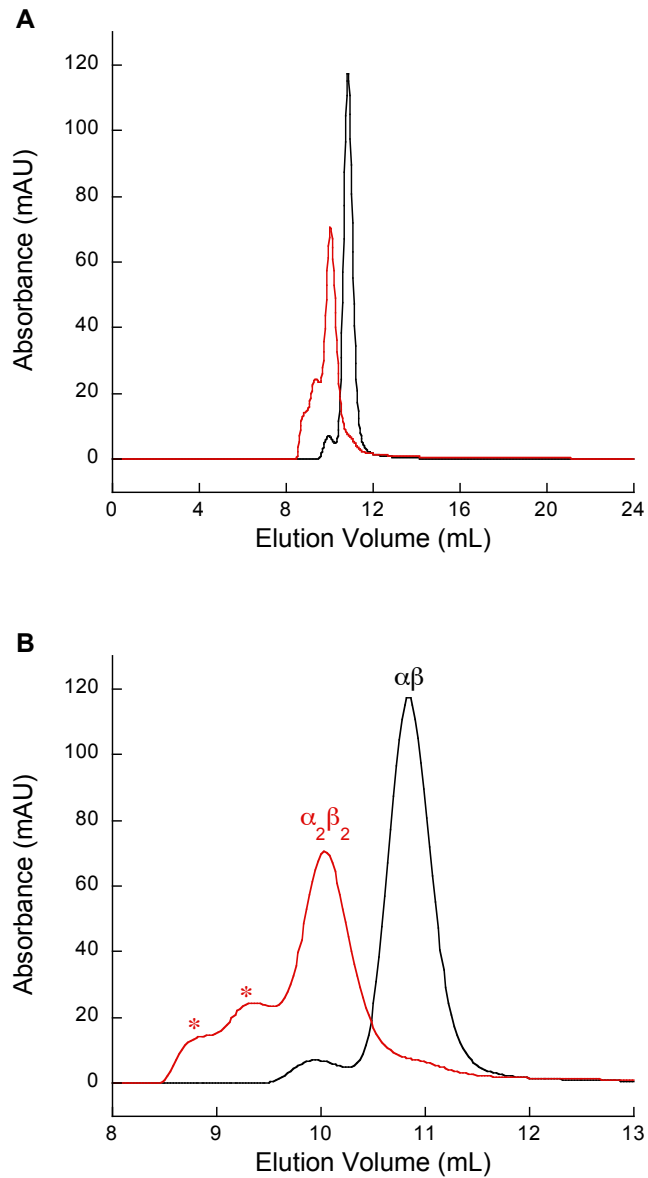


Figure S19. Analytical size exclusion chromatography of 100 μM CP-Ser ΔHis_4 in the absence (black) and presence (red) of 2 mM Ca(II) in the running buffer (75 mM HEPES, 100 mM NaCl, pH 7.5). **(A)** Full chromatograms. **(B)** Expansion. The red stars indicate Ca(II)-dependent peaks attributed to higher-order oligomers. Absorption was monitored at 280 nm and room temperature. Elution volumes are listed in Table S8.

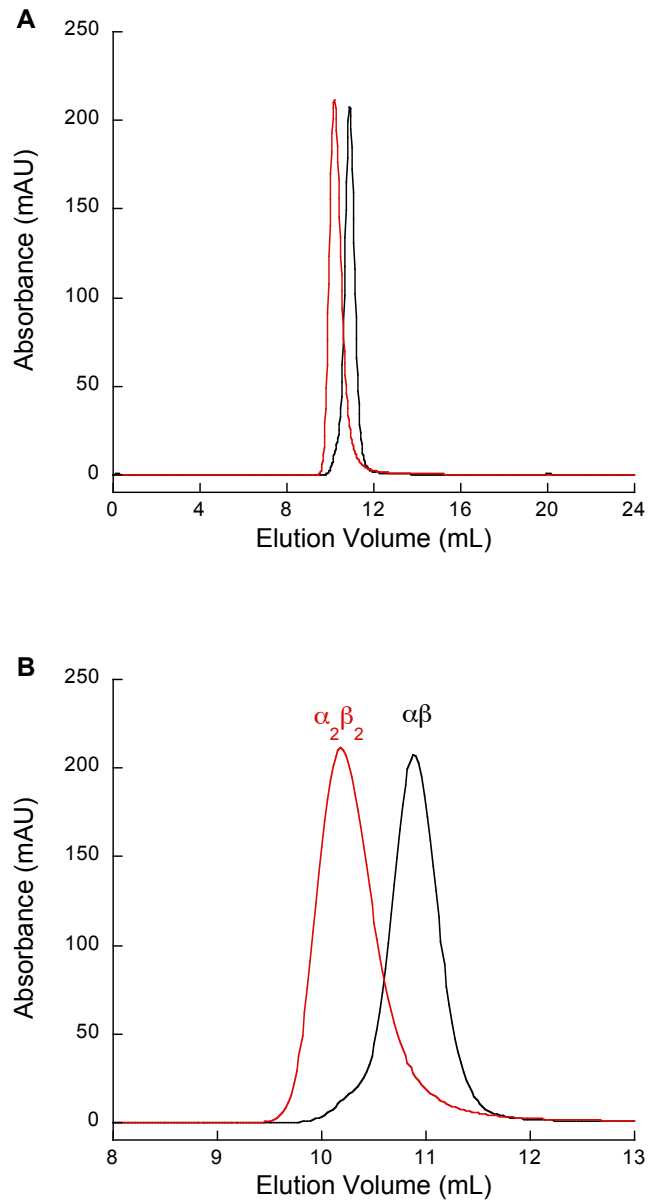


Figure S20. Analytical size exclusion chromatography of 100 μ M CP-Ser(H83A) in the absence (black) and presence (red) of 2 mM Ca(II) in the running buffer (75 mM HEPES, 100 mM NaCl, pH 7.5). **(A)** Full chromatograms. **(B)** Expansion. Absorption was monitored at 280 nm and room temperature. Elution volumes are listed in Table S8.

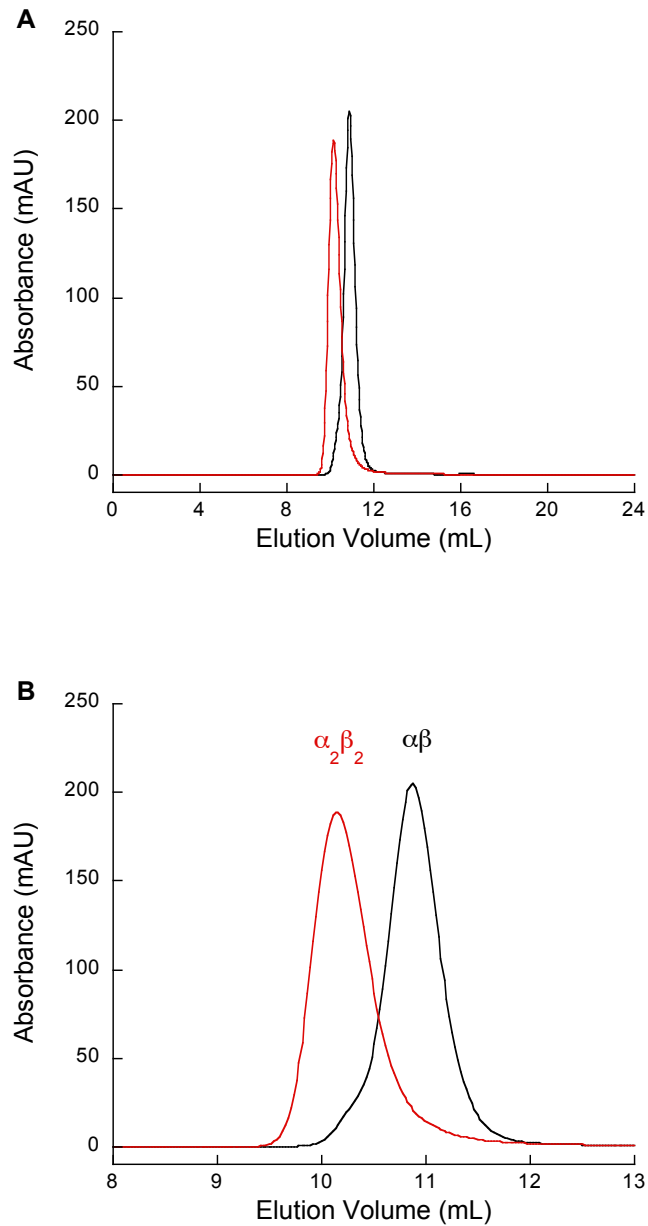


Figure S21. Analytical size exclusion chromatography of 100 μ M CP-Ser(H87A) in the absence (black) and presence (red) of 2 mM Ca(II) in the running buffer (75 mM HEPES, 100 mM NaCl, pH 7.5). **(A)** Full chromatograms. **(B)** Expansion. Absorption was monitored at 280 nm and room temperature. Elution volumes are listed in Table S8.

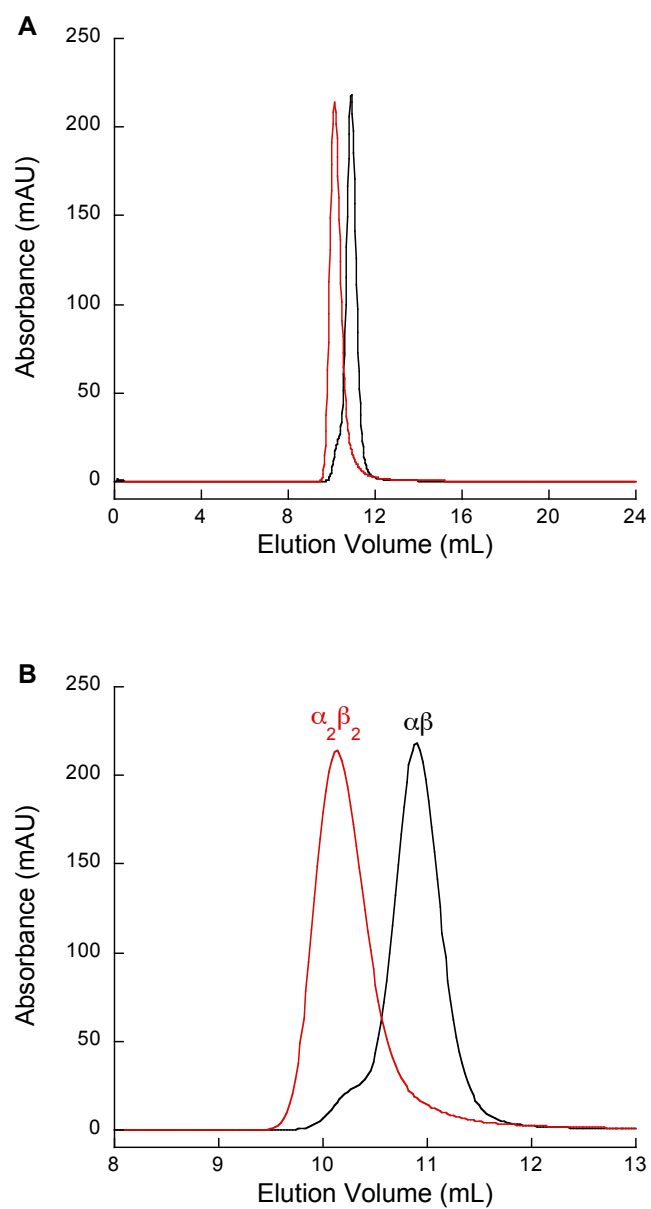


Figure S22. Analytical size exclusion chromatography of 100 μ M CP-Ser(H20A) in the absence (black) and presence (red) of 2 mM Ca(II) in the running buffer (75 mM HEPES, 100 mM NaCl, pH 7.5). **(A)** Full chromatograms. **(B)** Expansion. Absorption was monitored at 280 nm and room temperature. Elution volumes are listed in Table S8.

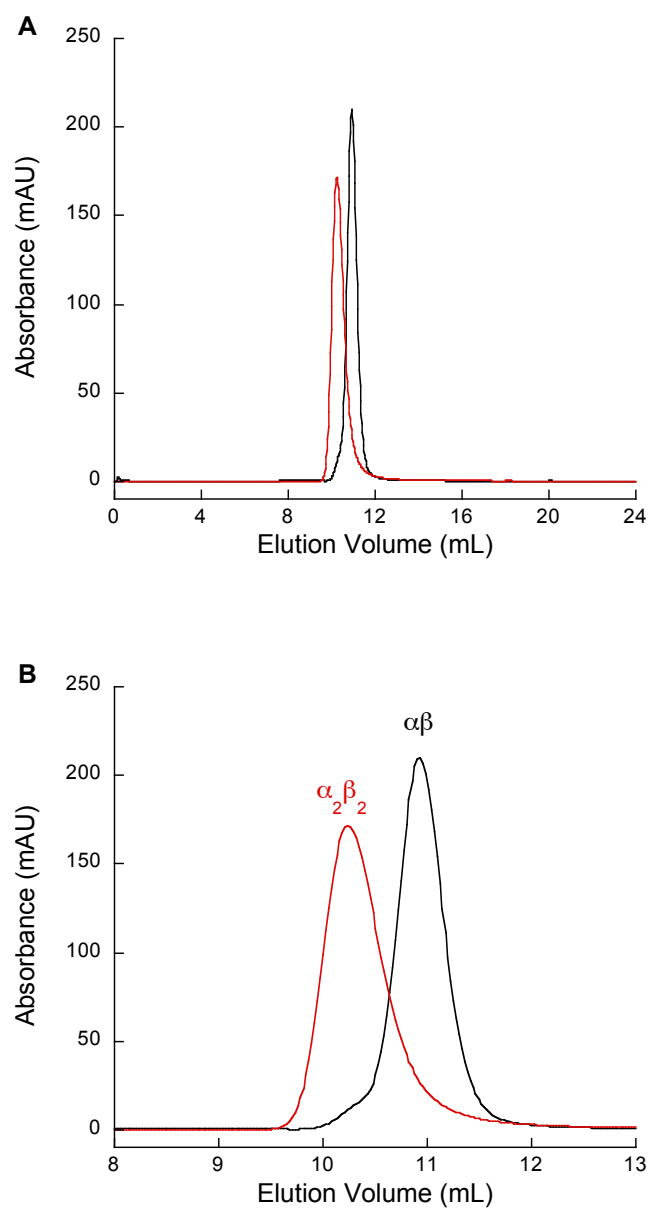


Figure S23. Analytical size exclusion chromatography of 100 μ M CP-Ser(D30A) in the absence (black) and presence (red) of 2 mM Ca(II) in the running buffer (75 mM HEPES, 100 mM NaCl, pH 7.5). **(A)** Full chromatograms. **(B)** Expansion. Absorption was monitored at 280 nm and room temperature. Elution volumes are listed in Table S8.

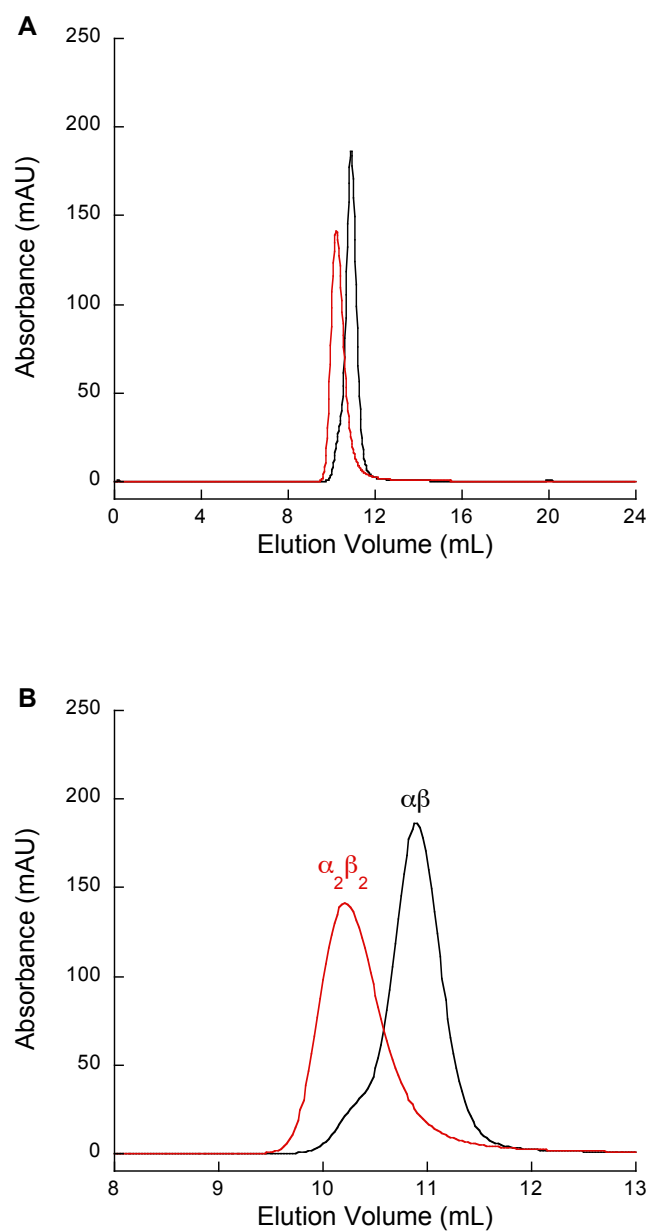


Figure S24. Analytical size exclusion chromatography of 100 μ M CP-Ser(D30A)(H83A) in the absence (black) and presence (red) of 2 mM Ca(II) in the running buffer (75 mM HEPES, 100 mM NaCl, pH 7.5). **(A)** Full chromatograms. **(B)** Expansion. Absorption was monitored at 280 nm and room temperature. Elution volumes are listed in Table S8.

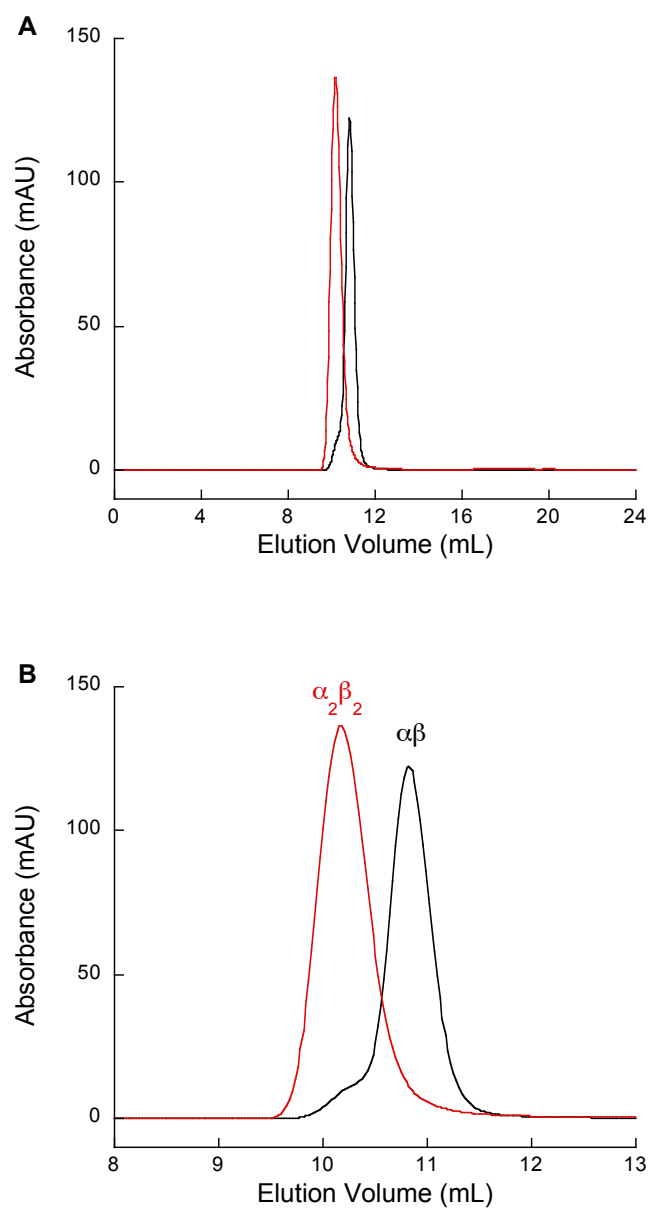


Figure S25. Analytical size exclusion chromatography of 100 μ M CP-Ser Δ His₃Asp in the absence (black) and presence (red) of 2 mM Ca(II) in the running buffer (75 mM HEPES, 100 mM NaCl, pH 7.5). **(A)** Full chromatograms. **(B)** Expansion. Absorption was monitored at 280 nm and room temperature. Elution volumes are listed in Table S8.

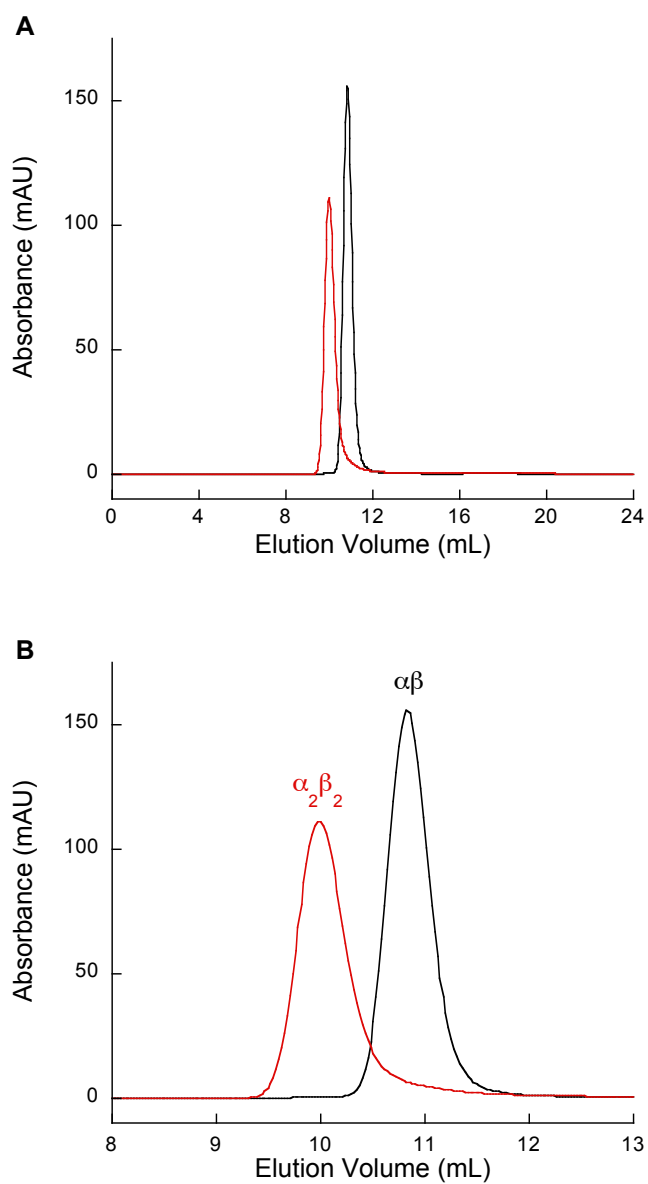


Figure S26. Analytical size exclusion chromatography of 100 μM CP-Ser $\Delta\Delta$ in the absence (black) and presence (red) of 2 mM Ca(II) in the running buffer (75 mM HEPES, 100 mM NaCl, pH 7.5). **(A)** Full chromatograms. **(B)** Expansion. Absorption was monitored at 280 nm and room temperature. Elution volumes are listed in Table S8.

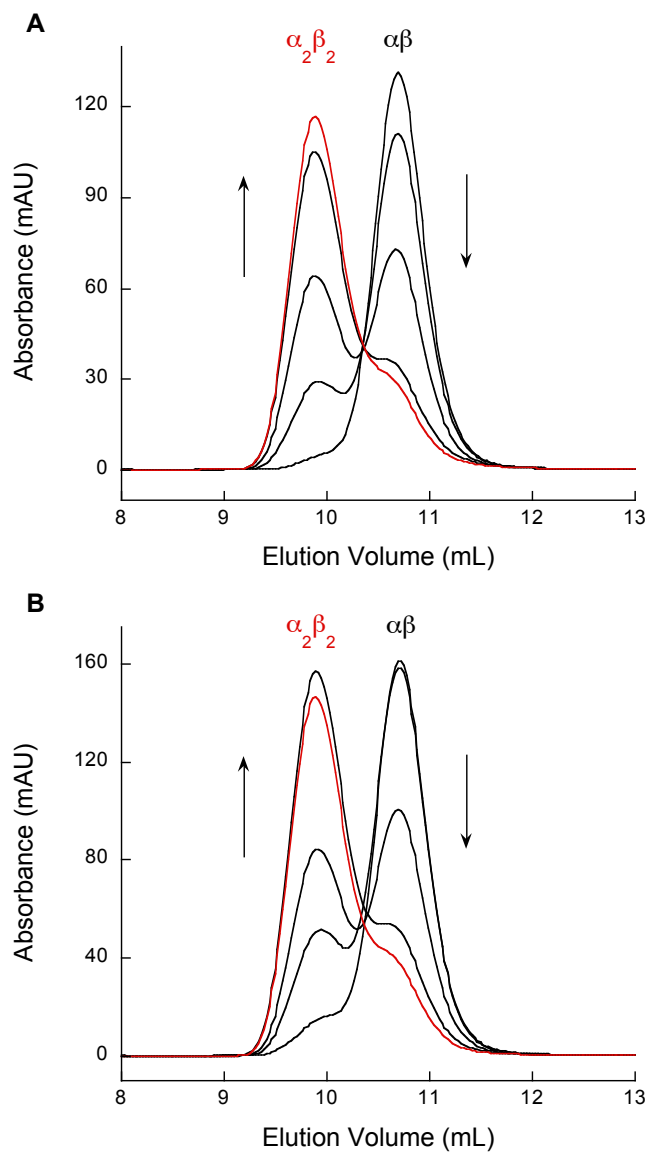


Figure S27. Calcium-binding titrations monitored by SEC at pH 8.0 (20 mM HEPES, 100 mM NaCl). **(A)** 135 μ M CP. **(B)** 122 μ M CP-Ser. CP was eluted following addition of 0, 1, 2, 4 and 8 equivalents of Ca(II). The absorbance was monitored at 216 nm and $T = 4$ °C.

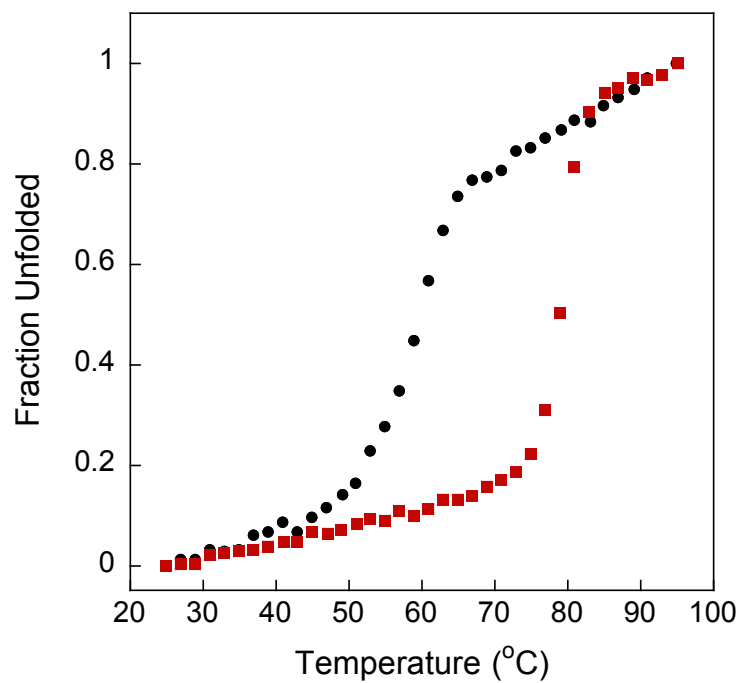


Figure S28. Thermal denaturation of 10 μ M CP-Ser at pH 8.5 (1 mM Tris, 0.5 mM EDTA) in the absence (black circles) and presence (red squares) of 2 mM Ca(II). Absorption at 222 nm was monitored. The denaturation curves afford T_m values of 59 °C and 79 °C in the absence and presence of Ca(II), respectively.

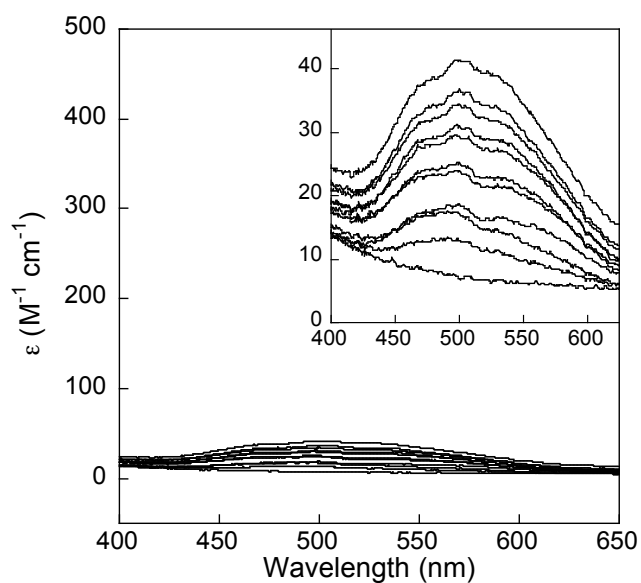


Figure S29. Titration of 400 μM CP-Ser $\Delta\text{His}_3\text{Asp}$ with 0 – 5 equiv of Co(II) monitored by optical absorption spectroscopy (75 mM HEPES, 100 mM NaCl, pH 7.0). This figure corresponds to Figure 3C of the main text and includes the inset showing an expanded y-axis version of the plot.

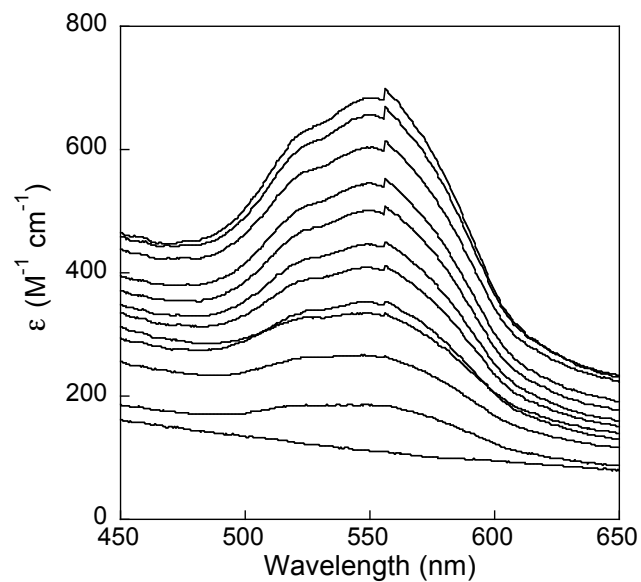


Figure S30. Titration of 100 μM CP-Ser with 0 – 3 equiv of Co(II) in the presence of 2 mM Ca(II) monitored by optical absorption spectroscopy (75 mM HEPES, 100 mM NaCl, pH 7.0). Precipitation occurred at higher equivalents of Co(II).

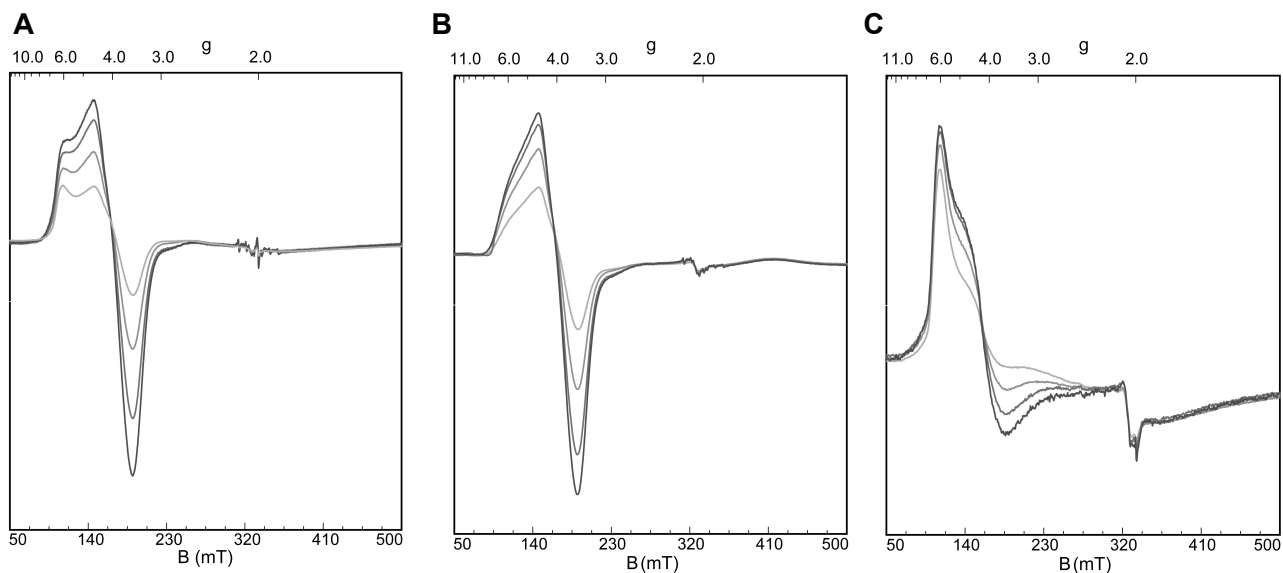


Figure S31. EPR power saturation experiments. **(A)** CP-Ser, reprinted from Figure 3A of the main text and shown here for comparison. **(B)** CP-Ser Δ His₃Asp. **(C)** CP-Ser Δ His₄. EPR spectra were recorded at 10.6 K with powers of 0.6 (dark grey), 2, 6, and 20 (light grey) mW. The samples contained 1.1 mM CP and 0.8 equivalents of Co(II) (20 mM HEPES, 100 mM NaCl, pH 7.0). Instrument conditions: temperature, 10.6 K; 9.38 GHz; modulation amplitude, 8.0 G.

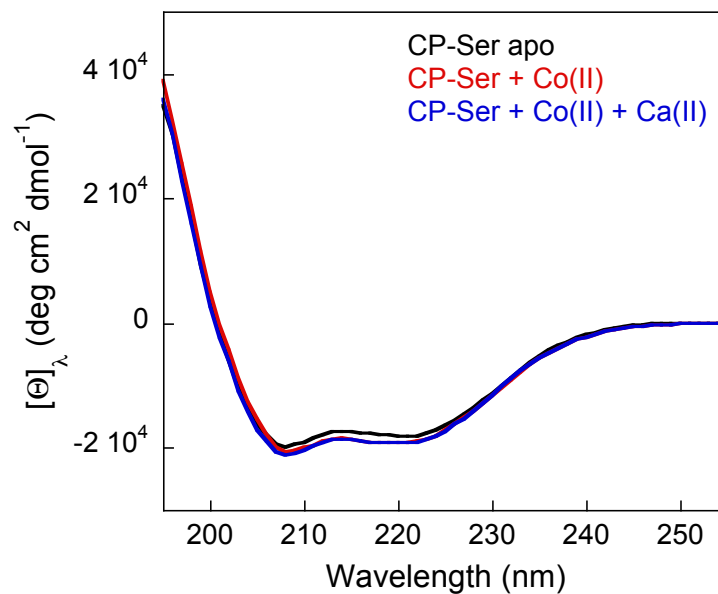


Figure S32. CD spectra of 10 μM CP-Ser in the absence and presence of 10 equiv of Co(II) at pH 7.5 (1 mM Tris). The black line is the CD spectrum of CP-Ser in the absence of any metal ions. The red line is the spectrum of CP-Ser in the presence of 10 equiv of Co(II). The blue line is the CD spectrum of CP-Ser in the presence of Co(II) and 2 mM Ca(II).

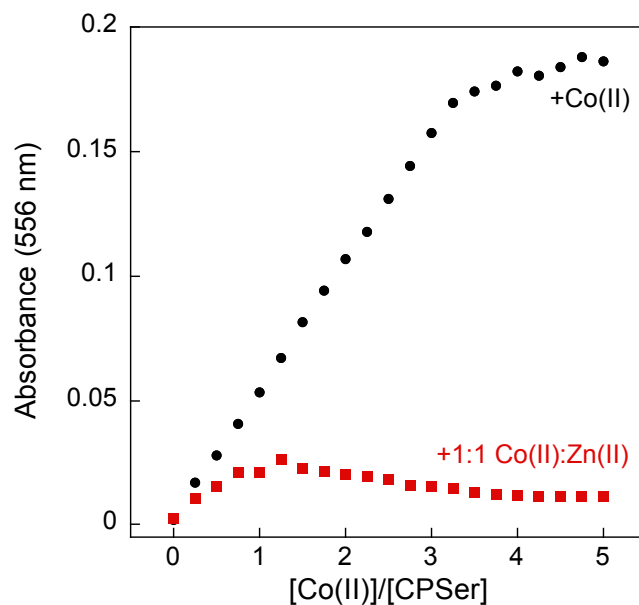


Figure S33. Titration of 400 μ M CP-Ser with Co(II) or a 1:1 mixture of Co(II):Zn(II) at pH 7.0 (75 mM HEPES, 100 mM NaCl) monitored by optical absorption spectroscopy ($T = 25\text{ }^{\circ}\text{C}$). The Co(II) titration data correspond to the optical absorption spectra presented in Figure 3A of the main text. Each optical absorption measurement was made ca. 1 min after addition of the metal solution to the cuvette.

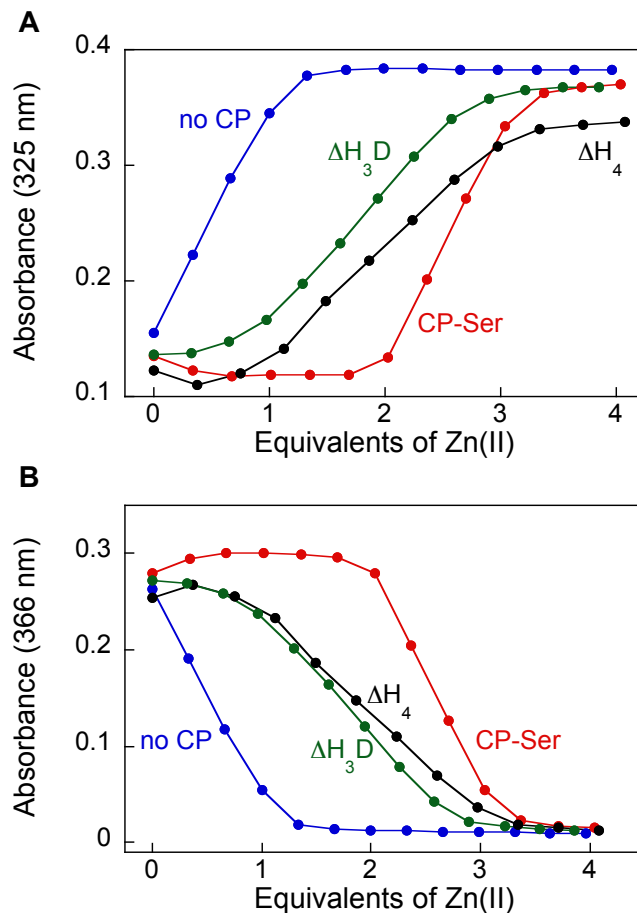


Figure S34. Response of 10 μM MF2 to Zn(II) in the presence of ca. 10 μM CP. **(a)** Absorption change at 325 nm. **(b)** Absorption change at 366 nm. The absorption values at 325 and 366 nm indicate that MF2 responds to Zn(II) after CP-Ser (9.8 μM) binds two equivalents or after the ΔHis_3 (8.6 μM) and $\Delta\text{His}_3\text{Asp}$ (10 μM) mutants each coordinate one equivalent of Zn(II). The x-axis refers to the Zn/CP for samples containing protein and the Zn/MF2 ratio for the titration conducted in the absence of CP.

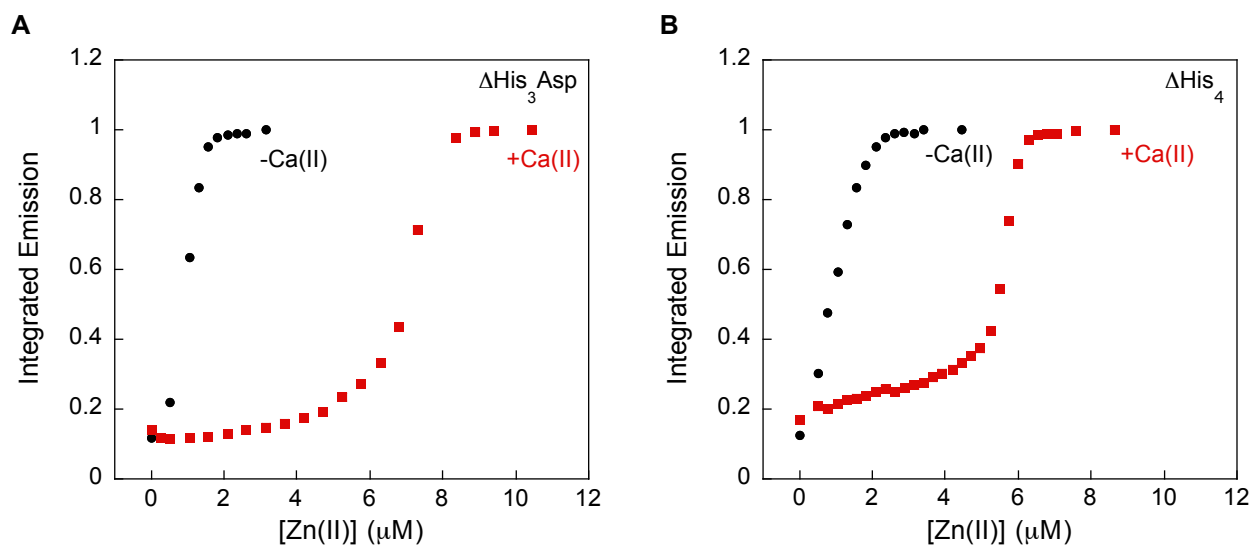


Figure S35. Fluorescence response of $\sim 2 \mu\text{M}$ ZP4 to Zn(II) in the presence of CP-Ser $\Delta\text{His}_3\text{Asp}$ and ΔHis_4 . **(A)** Response of ZP4 to Zn(II) in the presence of $\Delta\text{His}_3\text{Asp}$. Black circles: $11.2 \mu\text{M}$ CP-Ser $\Delta\text{His}_3\text{Asp}$, no added calcium. Red squares: $9.9 \mu\text{M}$ $\Delta\text{His}_3\text{Asp}$ and in the presence of $200 \mu\text{M}$ Ca(II). **(B)** Response of ZP4 to Zn(II) in the presence of ΔHis_4 . Black circles: $7.9 \mu\text{M}$ ΔHis_4 , no added calcium. Red square: $7.6 \mu\text{M}$ ΔHis_4 and in the presence of $200 \mu\text{M}$ Ca(II). All titrations were conducted at pH 7.5 (75 mM HEPES, 100 mM NaCl) and at 25°C . Excitation was provided at 495 nm and the emission spectra were integrated from 500 – 650 nm.

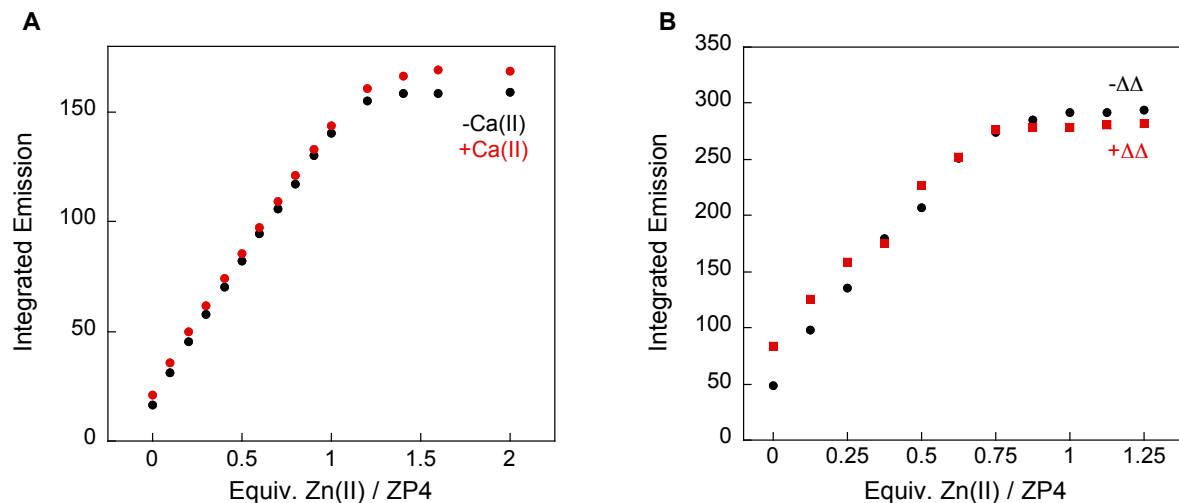


Figure S36. The fluorescence response of ZP4 to Zn(II) is unaffected by Ca(II) and CP $\Delta\Delta$. **(A)** Titration of 2 μM ZP4 with Zn(II) in the absence (black circles) and presence (red squares) of 500 μM Ca(II). The presence of Ca(II) has no effect on the response of ZP4 to Zn(II). **(B)** Fluorescence response of 1.6 μM ZP4 to 0 – 1.4 equivalents of Zn(II) in the absence and presence of 10 μM CP-Ser $\Delta\Delta$. Black circles: Titration of ZP4 with Zn(II) in the absence of $\Delta\Delta$. Red squares: Titration of ZP4 with Zn(II) in the presence of 10 μM CP-Ser $\Delta\Delta$. All titrations were conducted at pH 7.5 (75 mM HEPES, 100 mM NaCl) and 25 $^{\circ}\text{C}$. Excitation as provided at 495 nm and the spectra were integrated from 505-650 nm.

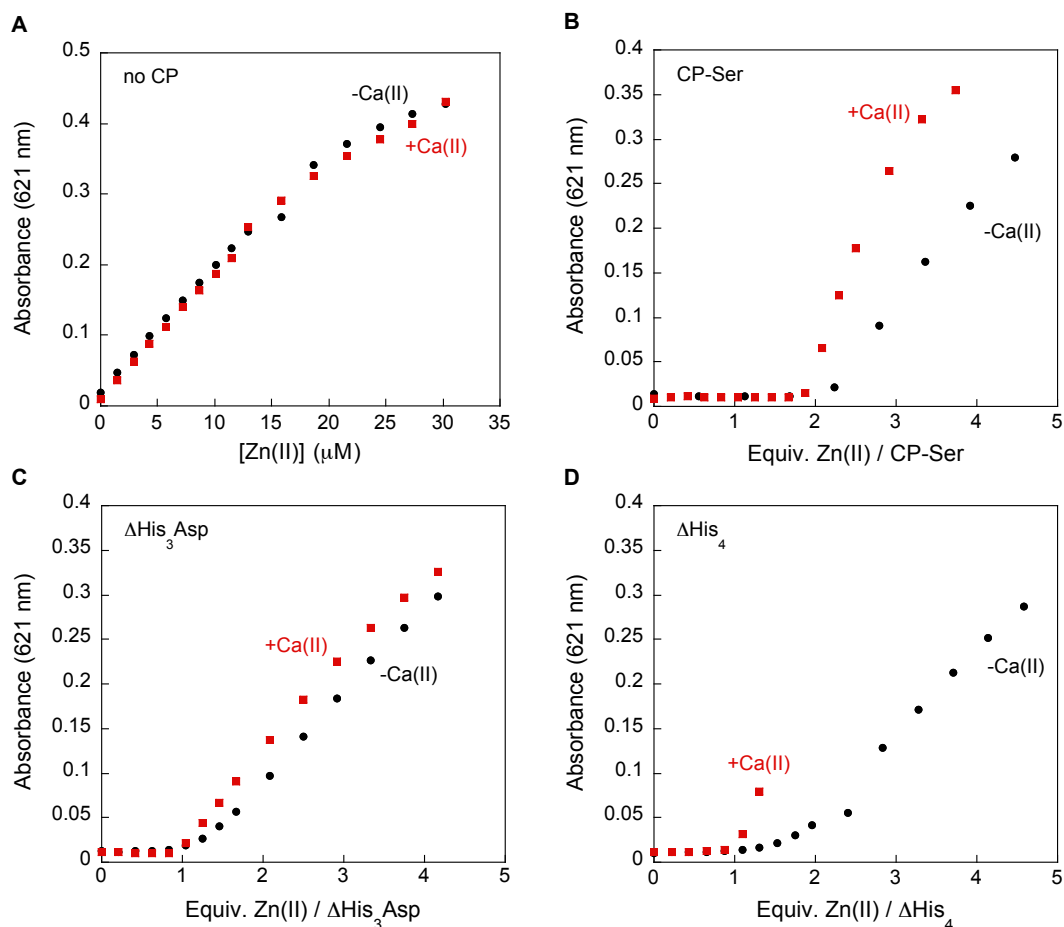


Figure S37. Response of Zincon to Zn(II) in the presence of CP and Ca(II). **(A)** Response of 25 μM Zincon to Zn(II) in the absence (black circles) and presence (red squares) of 200 μM Ca(II). The presence of Ca(II) has negligible effect on the Zincon response. **(B)** Response of 25 μM Zincon to Zn(II) in the presence of CP-Ser and in the absence (black circles, 9.9 μM CP) and presence (red squares, 17.7 μM CP) of 200 μM Ca(II). The break at 2 indicates that CP-Ser binds Zn(II) with 2:1 Zn:CP stoichiometry in the absence and presence of excess Ca(II). **(C)** Response of 25 μM Zincon to Zn(II) in the presence of 6.9 μM CP-Ser ΔHis₃Asp and in the absence (black circles) and presence (red squares) of 200 μM Ca(II). **(D)** Response of 25 μM Zincon to Zn(II) in the presence of 6.6 μM CP-Ser ΔHis₄ and in the absence (black circles) and presence (red squares) of 200 μM Ca(II). Precipitation occurred during the titrations of ΔHis₄ in the presence of Ca(II). The breaks at 1 indicate that ΔHis₃Asp and ΔHis₄ bind Zn(II) with 1:1 Zn:CP stoichiometry in the absence and presence of excess Ca(II).

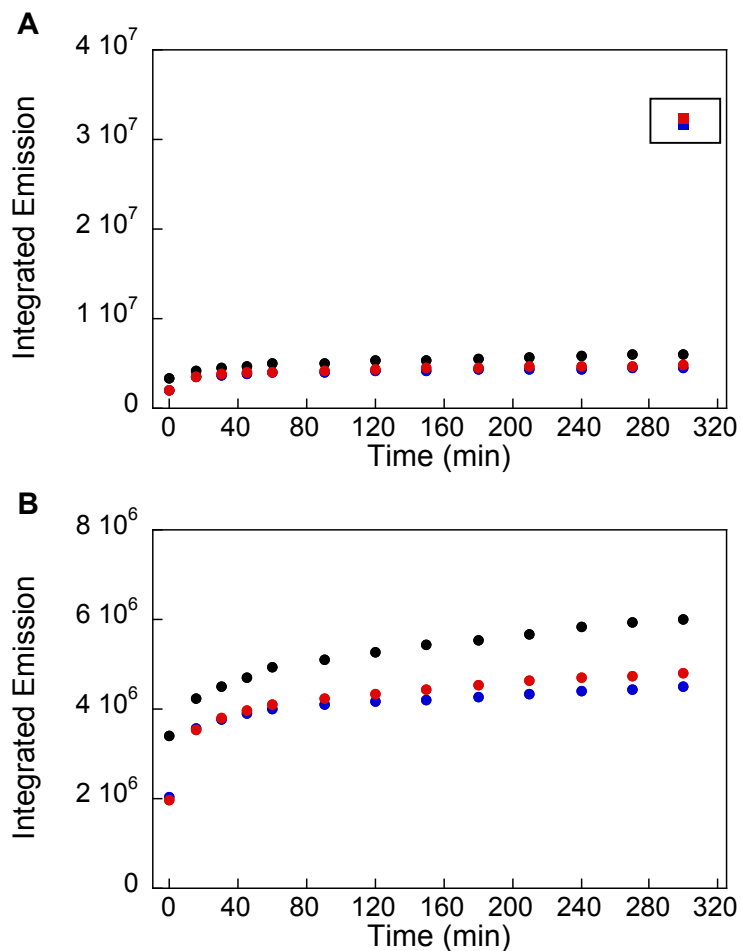


Figure S38. Fluorescence emission from 1.9 μM ZP4 in the presence of 1:2 Zn(II):CP-Ser. **(A)** ZP4 was added to a solution containing ca. 4 μM Zn(II) and ca. 8 μM CP-Ser and the emission spectra were recorded over the course of 300 min. Black circles, ZP4 only; blue circles, ZP4 and CP-Ser; red circles, ZP4 and 1:2 Zn(II):CP-Ser. The changes in ZP4 emission under all experimental conditions are comparable. Boxed data points: addition of 50 μM Zn(II) to the solutions at $t = 300$ min resulted in ZP4 turn-on. **(B)** Expansion of the y-axis. The experiments were conducted at pH 7.5 (75 mM HEPES, 100 mM NaCl) and at 25 $^{\circ}\text{C}$. Excitation was provided at 495 nm and the emission spectra were integrated from 500 – 650 nm.

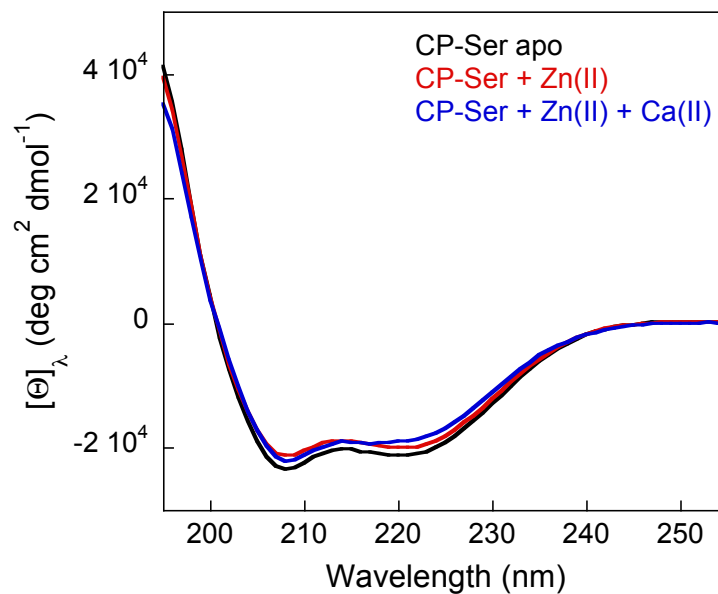


Figure S39. CD spectra of 10 μM CP-Ser in the absence and presence of three equivalents of Zn(II) at pH 7.5 (1 mM Tris). The black line is the CD spectrum of CP-Ser in the absence of any metal ions. The red line is the spectrum of CP-Ser in the presence of three equivalents of Zn(II). The blue line is the CD spectrum of CP-Ser in the presence of Co(II) and 2 mM Ca(II).

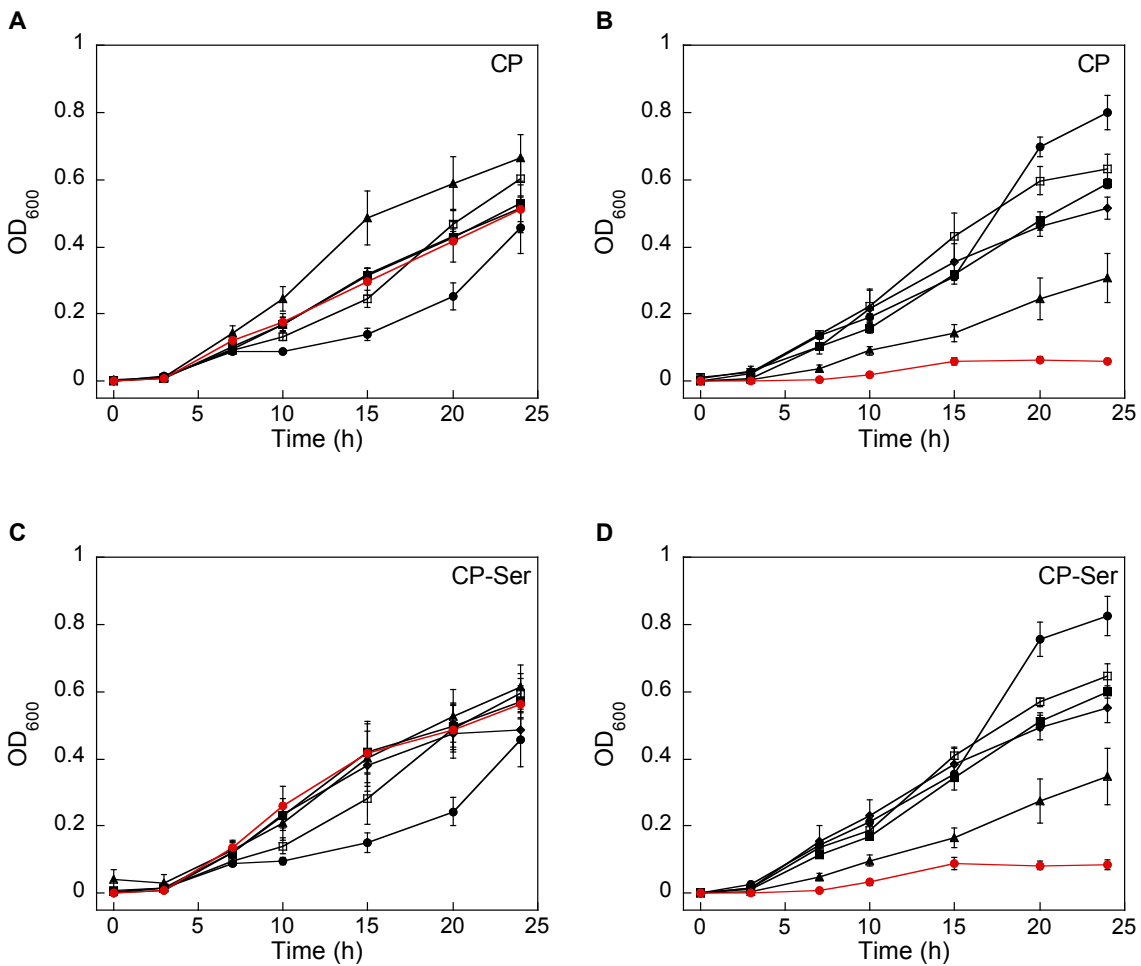


Figure S40. Growth inhibitory activity of CP and CP-Ser against *Staphylococcus aureus* ATCC 25923 in the absence and presence of a 2 mM Ca(II) supplement as described in the main text. (A) Wild-type CP in the absence of added Ca(II). (B) Wild-type CP in the presence of 2 mM Ca(II). (C) CP-Ser in the absence of added Ca(II). (D) CP-Ser in the presence of added Ca(II). Black circles, 0 $\mu\text{g/mL}$ CP; open squares, 31.25 $\mu\text{g/mL}$ CP; black diamonds, 62.5 $\mu\text{g/mL}$ CP; black squares, 125 $\mu\text{g/mL}$ CP; black triangles, 250 $\mu\text{g/mL}$ CP; red circles, 500 $\mu\text{g/mL}$ CP.

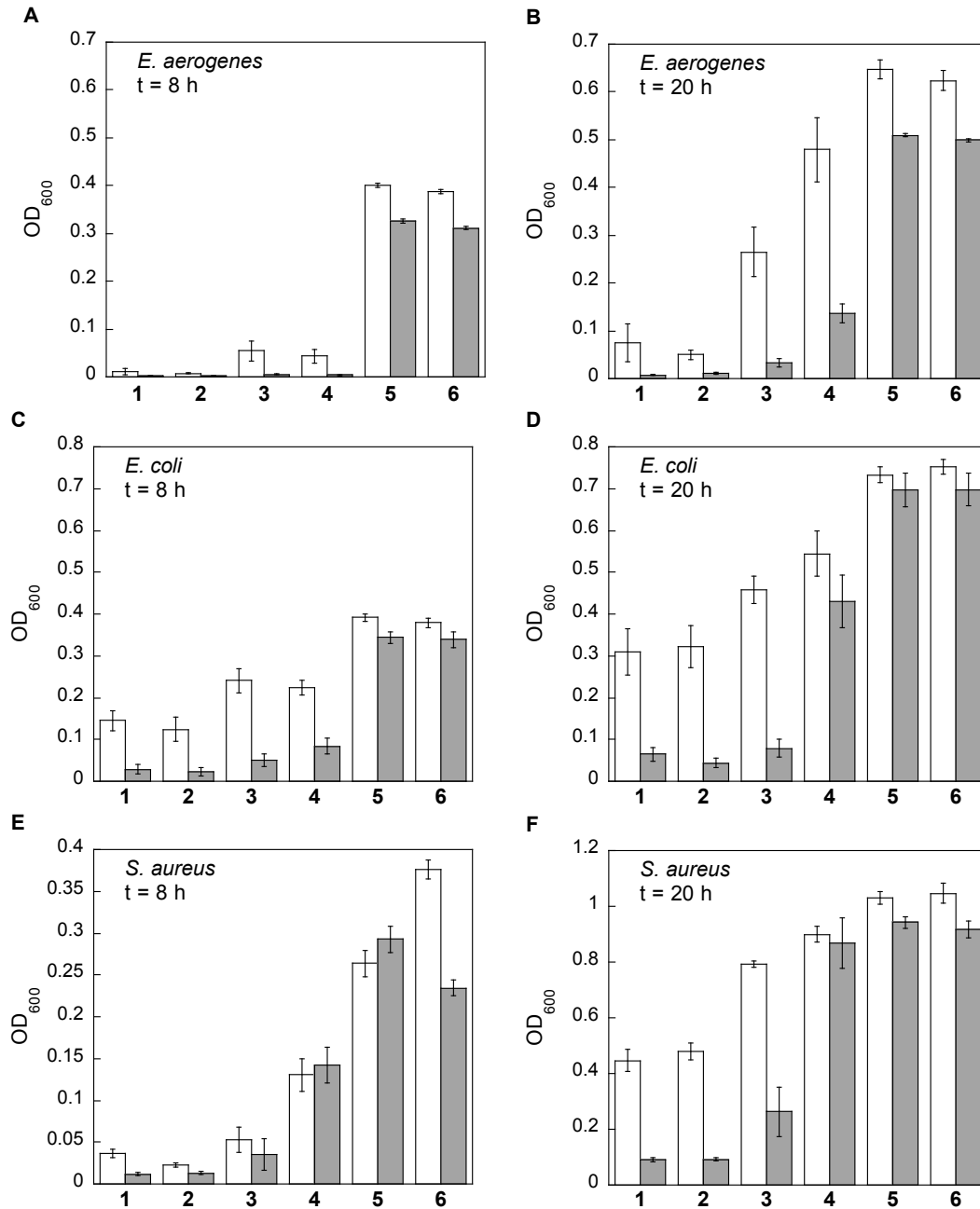
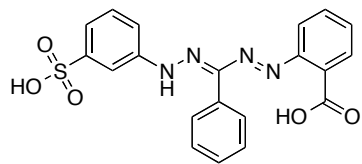
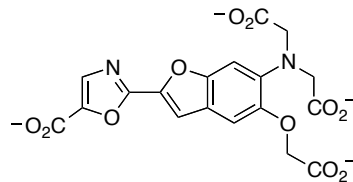


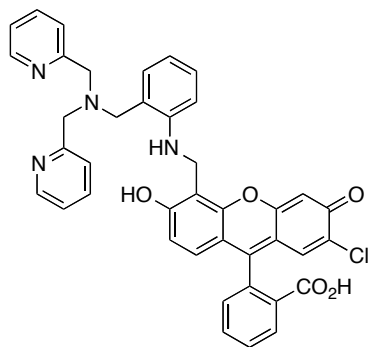
Figure S41. Synergistic effect of CP and β -mercaptoethanol (BME) on bacterial growth inhibition. Bacterial cultures were treated with 500 $\mu\text{g}/\text{mL}$ CP and incubated at 30 $^{\circ}\text{C}$ with shaking in growth medium with (grey bars) or without (white bars) 3.1 mM BME (final concentration). The OD₆₀₀ values were recorded at t = 8 and t = 20 h. **1**, wild-type CP; **2**, CP-Ser, **3**, $\Delta\text{His}_3\text{Asp}$; **4**, ΔHis_4 ; **5**, $\Delta\Delta$; **6**, buffer only. **(A)** *E. aerogenes*, t = 8 h; **(B)** *E. aerogenes*, t = 20 h; **(C)** *E. coli*, t = 8 h; **(D)** *E. coli*, t = 20 h; **(E)** *S. aureus*, t = 8 h; **(F)** *S. aureus*, t = 20 h.



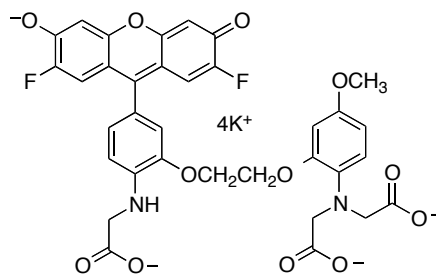
Zincon



Mag-Fura-2 (MF2)



Zinpyr-4 (ZP4)



FluoZin-3 (FZ3)

Figure S42. Structures of the colorimetric and fluorescent Zn(II) sensors employed in this study.